ONLINE SAG MILL PULSE MEASUREMENT AND OPTIMIZATION SEMI-ANNUAL TECHNICAL PROGRESS REPORT

Semi-annual Technical Report

Reporting period starting date December 24, 2005
Reporting period ending date June 24, 2006

RAJ RAJAMANI, PROJECT MANAGER
JOSE DELGADILLO, PROJECT LEADER
VISHAL DURISETI, GRADUATE STUDENT

Date report issued November 13, 2006

DEO Award number : DE –FC26-04NT42088

University of Utah
Metallurgical Engineering Department
135 South 1460 East Room 412
Salt Lake City, Utah 84112

DISCLAIMER

ABSTRACT

The grinding efficiency of semi autogenous milling or ball milling depends on the tumbling motion of the total charge within the mill. Utilization of this tumbling motion for efficient breakage of particles depends on the conditions inside the mill. However, any kind of monitoring device to measure the conditions inside the mill shell during operation is virtually impossible due to the sever environment presented by the tumbling charge. An instrumented grinding ball, which is capable of surviving a few hours and transmitting the impacts it experiences, is proposed here. The spectrum of impacts collected over 100 revolutions of the mills presents the signature of the grinding environment inside mill. This signature could be effectively used to optimize the milling performance by investigating this signature's relation to mill product size, mill throughput, make-up ball size, mill speed, liner profile and ball addition rates. At the same time, it can also be used to design balls and liner systems that can survive longer in the mill. The technological advances made in electronics and communication makes this leap in instrumentation certainly viable. Hence, the instrumented grinding ball offers the ability to qualitatively observe and optimize the milling environment.

LIST OF GRAPHICAL MATERIAL

TABLE OF CONTENTS

EXECUTIVE SUMMARY

The testing of the load cell on the ultra fast load cell assembly was a key experiment in designing the wireless circuit. The test worked showed that the load cell registered a peak force value upon a single impact within 100 microseconds. Since the impacts on the load cell package inside the mill can occur at any number of random times the demand on the wireless circuit is that it must gather data faster than 100 microsecond interval between two data points.. Hence, after much testing with vendor supplied wireless monitors, a decision was made to design and fabricate our own wireless monitor.

Ultra Fast Load Cell (UFLC) was developed at the Utah Comminution Center to measure this kind of high-speed single particle breakage events,. To understand the variation in the peak force experienced, several experiments were performed varying the ball size (which is equivalent to varying the mass) and the drop height. All of the results are in order to proceed ahead.

The data from UFLC was used to test the accuracy of the data generated from the new sensor installed in the IGB. Drop-ball tests were performed on the sensor-package under similar conditions as on the UFLC, and the data was found to be a very sound.

Several experiments were performed in an 8.5 x 9 inch laboratory scale ball mill. This set up is meant for finding problems with the sensor package and improving on it, and hence the wiring and components were installed for ease of removal and reinstallation. Ball size of 1.28 inch was used at 28% mill filling. The mill was run for 4, 8, 12, 16 and 20 minutes at 60%, 70% and 80% critical speed. The data was collected on a continuous basis and force spectrum and the force histogram were generated for each run.

The histogram shown here paves the way for SAG mill signature. In other words, a SAG mill would exhibit a specific force histogram under a set of operating conditions.

The IGB was tested in the SAG mill at Cortez Gold Mines Operations. Even though the device worked well it could not withstand the impacts in the plant scale mill. A decision was made to incorporate the load sensor package outside the mill, away from the severe impacting zone. Accordingly, back at the University development work began on an integrated package that could be mounted to the lifter bolts protruding outside the cylindrical mill frame.
The integrated load sensor package took three revisions to over come mechanical and vibration problems. Finally this package began to work well in a pilot scale (0.42 X 0.63 m) mill. A number of experiments were conducted to test the robustness and accuracy of the package. The net result is that the package performs very well.
Currently we are building the package that would fit on the 1.75 inch lifter bolt of the Cortez SAG mill. A specialized testing rig is being built to test such a large load cell package. Also, we have advanced our wireless capability to 2.4GHz with a Aerocomm board. In the next quarter we will be testing this unit in the Cortez SAG mill.

1. INTRODUCTION

Comminution can be defined as the process by which materials are reduced in size. Typically it is performed in two steps –Crushing and Grinding. Grinding is the last stage of comminution in which the particles are reduced in size by a combination of impact and abrasion, either dry or in slurry with water. It is performed in rotating cylindrical steel vessels known as tumbling mills, most common of them being ball mills, rod mills, autogenous mill and semiautogenous mills. These contain a charge of loose crushing bodies – the grinding medium – which is free to move inside the mill, thus comminuting the ore particles. The grinding medium constitutes steel balls or rods, hard rock and in some cases ore itself. The mill is rotated with a certain speed to get the stipulated ground product. Often, in the grinding process, particles between 5 and 250mm are reduced to 10 and 300μm. Grinding is the most energy intensive unit operation in mineral processing industry. It has been estimated that 50% of the energy consumption in metal extraction is used in comminution.

Much work has been devoted throughout the last century to improve the process of comminution. Most efforts have been focused on the design of new and more efficient size reduction equipment, optimization of the performance of existing equipment, and computer control. Some successful results of these efforts are the full scale development of autogenous, semiautogenous mills, vibratory grinding mills and more recently the high-pressure grinding roll mill. Also, great success has been achieved through the application of modern control techniques to industrial grinding circuits.

Current, semiautogenous and ball mills expend approximately 99 trillion Btu's annual for size reduction. Comminution in grinding mills is inherently inefficient using only about 1 percent of the input energy. Grinding mills also consume tons of steel balls and liners. By monitoring grinding mill operation, grinding energy efficiency can be improved by as much as 10 percent.

Figure 1.1 Industrial SAG mill

Many large mining operations have one or more semi-autogenous (SAG) mills doing bulk of the work in their size reduction operation. The SAG mill performance is determined by a large number of variables, both mine site variables and mill variables. In many cases these variables dictate production capacity seemingly randomly. The mill variables can be broadly put into two groups related to 1) the grinding chamber and 2) the discharge section, whose schematic is shown in Figure 1.2.

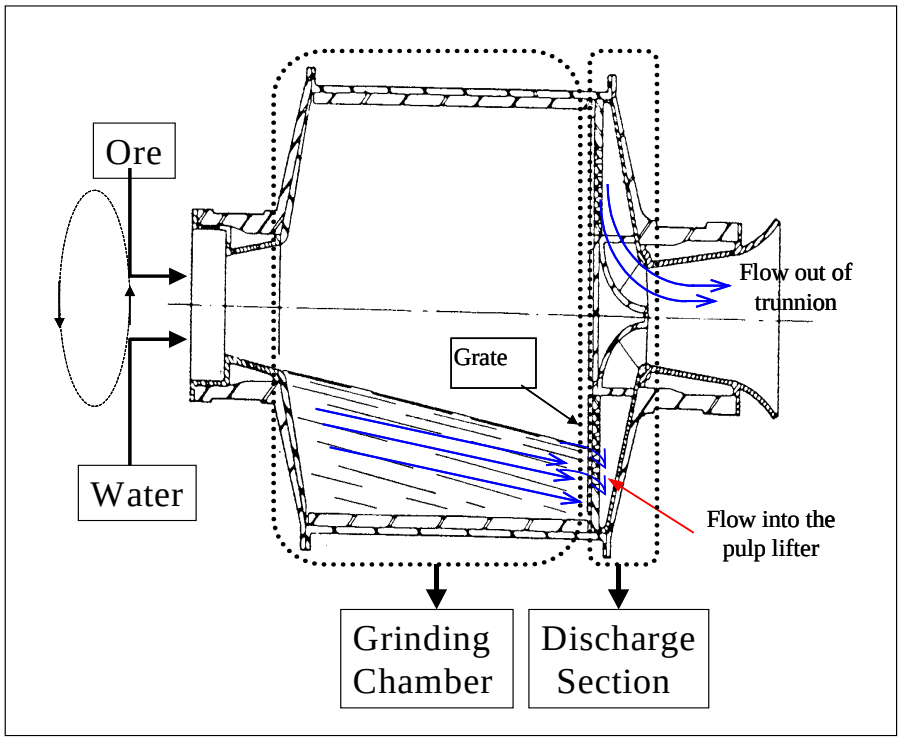

Figure 1.2 Schematic of a semiautogenous mill

The grinding chamber is the place where breakage of particles occurs due to the tumbling motion of the grinding balls and ore particles. The optimal design of shell lifters can produce an efficient charge motion. Once the discharge grate and pulp lifters are designed properly for the required mill capacity, they would perform consistent with the overall design. However, the milling conditions inside the grinding chamber keep changing. The change is mainly due to the mine variables and wearing of shell liners (lifters) with time. Till date these uncontrollable and dynamic variations are interpreted based on the power draft and in some operations with load cells readings. More recently, mill sound recording is also are also used to infer online the dynamics of the mill. All these techniques are the indirect ways of the milling conditions inside the mill.

The best approach till date to predict the charge motion in a mill is by using Discrete Element Method (DEM) based simulations. The DEM is a way of modeling the motions and interactions of a set of individual particles and moving walls, as affected by gravity, models for particle interaction and Newton's Laws of Motion. The interactions of the particles are modeled by the spring-slider-dashpot model. The particle and wall material properties are taken into account by specifying the coefficients of friction and restitution, as well as the shear and normal stiffness.

It is only due to the recent advances in computer accessibility and speed that it has become viable to calculate the motion of large sets of interacting particles. At first, a two-dimensional slice of the grinding mill, was simulated (2D DEM). This assumed that there was little net motion in the third dimension. With faster computers becoming available at reasonable cost, the developers of DEM software are rapidly turning to three-dimensional simulations (3D DEM).

To date most validation of DEM applied to grinding mills has been to compare the power drawn by mills and overall load motion. Good predictions of mill power do not necessarily imply that the DEM provides a reliable model for mill behavior. There are a number of possible load behavior conditions that could result in the same power drawn. However, all energy provided to the load is passed through the mill shell. Thus the forces on a lifter would give a more detailed indication of how power is provided.

It is essential that DEM predictions will be verified rigorously against experimental data. It is only once DEM has been shown to model the load behaviour adequately that the predictions will be used with confidence in industrial applications.

An instrumented load cell package, which is capable of surviving a few hours and transmitting the impacts it experiences, is developed here. The spectrum of impacts collected over 100 revolutions of the mills presents the signature of the grinding environment inside mill. This signature could be effectively used to optimize the milling performance by investigating this signature's relation to mill product size, mill throughput, make-up ball size, mill speed, liner profile and ball addition rates. At the same time, it can also be used to design balls and liner systems that can survive longer in the mill.

With the load cell package, the impact spectrum of an operating mill can be measured. It is important to interpret the spectrum in terms of the mill's operating efficiency. The typical spectrum shown in Figure 1.3 is expected to be a bell-shaped curve centered on the average impact force. The left-hand side corresponds to lower energy impacts whereas the right side denotes the high energy impacts. The average value typifies the force regime in the mill. High impacts reflect on the cataracting action in the mill, and low impacts reflect on the ratio of rock mass to ball mass as well as the cascading action in the mill. The spectrum is greatly affected by the wear of the lifters and the make-up of the charge mass. By comparing the spectrum with that obtained during best operating conditions, one is able to take control actions and keep the mill at its highest throughput rate.

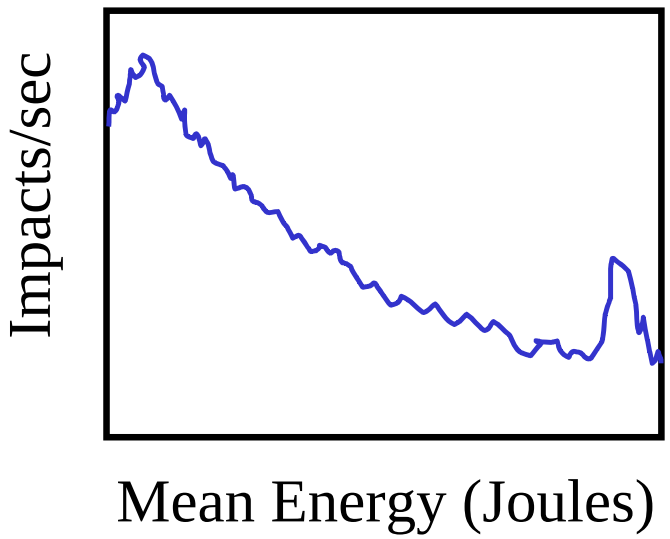

Figure 1.3 A typical Impact spectra-the signature, generated in PC

The instrumented load cell package also greatly helps the grinding ball manufacturer and the lifter manufacturer in making balls and lifters capable of withstanding the intensity of grinding action in a particular operation. Using the observed impact spectrum, the manufacturer can tailor the alloy or composition or phase/grain structure of the steel to withstand the forces generated in a particular milling operation.

2 RESEARCH BACKGROUND

2.1 Literature Review

2.1.1 Sensors for Tumbling Mills

Monitoring grinding operation in tumbling mills has been the focus of research in academia and industry for several decades due to expectation of high throughput and low operating costs. Sensors form one of the main components of a successful monitoring system. Many different types of sensors have been commercially available. In milling systems, sensors are typically used to monitor ore hardness, particle size distribution, solid and liquid flow, mill noise, power draft, etc. Sensors come in a wide variety that can be categorized as direct, indirect, and soft sensors. For example, the strain gauges that are used as direct sensors are typically mounted inside the lifters and liners of the tumbling mill to measure the stress intensity on the mill shell. On the other hand, the indirect sensors that include acoustic sensors (non-contact type) are used to predict the state of grinding, wear of liners, etc.

2.1.1.1 Direct Sensors

In this category, sensors are typically designed for direct measurement of unknown process parameters of interest. For example, mechanical sensors that rely on magneto-elastic effects such as strain and force sensor, torque sensor, and displacement sensor are considered as direct sensors.

2.1.1.1.1 Power

Monitoring power consumption represents one of the simplest methods of monitoring the grinding efficiency. The power data has been successfully interpreted to correlate with mill capacity. But the main drawback is that in case of large industrial mills, small changes in the load or capacity cannot be detected through variations in power draw pattern. Nevertheless, the standard practice is to maximize mill power for maximum throughput. In many operations the maximizing mill power for maximum throughput works because it is believed that the greater the energy spent per unit mass the greater is the capacity or the smaller is the product size. In several situations this idea fails because the ore hardness changes too often. For example when a harder ore is fed to the mill, desired grinding is not achieved and material builds up inside the mill. As a result the power draw increases as grinding progresses.

2.1.1.1.2 Particle size distribution

It has been recognized in the mineral processing industry that on-line monitoring of the particle size distributions can provide crucial information for mill control. Unfortunately due to the difficulties in handling large tonnages, it is not possible to

perform on-line analysis from process streams such as the feed and recycle streams in a SAG mill or from crusher product streams using traditional sizing methods. Lately, online digital size analysis using video input has made it possible to monitor and even control the feed size to the mill. The procedure for the determination of rock size distribution on a conveyor that feeds the mill involves several stages of image processing.

2.1.1.1.3 Charge motion

In the last decade much has been learned about charge motion in tumbling mills. With the help of discrete element method (DEM) the effect of operating variables on the overall motion of the charge is fairly well understood. The relationship between impact spectra and breakage in the mill is evolving. Much has been also learnt about redesigning of liners and lifters. However, in SAG mills there is an ever pressing demand for online prediction of charge dynamics, charge constitution, and impact energy spectra.

Powell and Nurick (1996) traced the trajectory of a single ball that contained a radioactive source and filmed its path with a gamma-ray camera. These individual ball trajectories led to an understanding of charge interaction, charge segregation, and the influence of lifters. In a more ambitious approach Rajamani et al. (1996) photographed the motion of the charge in a pilot-scale mill. A camera was placed on a mechanically driven trolley that was periodically introduced from the feed end to capture an image of the charge. Figure 2.1 shows the camera location with respect to the feeding chute and a snapshot of the charge in motion. Several such snapshots can be processed to determine the ratio of amount of ball to rock. However to date, this technology has not evolved into a commercial application.

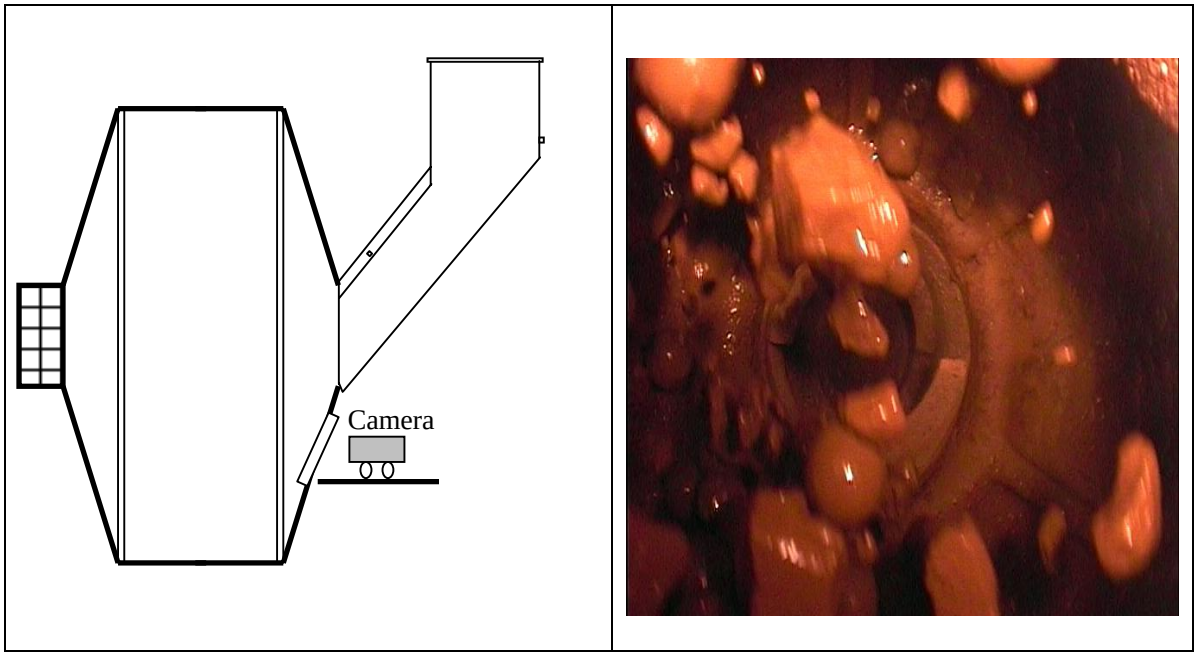

Figure 2.1 Right: arrangement of camera; Left: photograph of charge motion in a pilot scale mill.

2.1.1.2 Indirect measurement

2.1.1.2.1 Acoustic emission (AE) sensor

In several mineral-processing plants acoustic emission (AE) sensors are used. It is considered to be one of the most practical technologies to use for monitoring of mill operations and AE sensors have particularly made their way into SAG mill operations. Major conditions to be monitored and detected are intensity and type of impacts i.e., ball-ball and ball-liner. For the practical application of the AE sensor for monitoring of impacts, the first problem to be solved is how the sensor should be mounted on the mill. These sensors (one to four) are located roughly around 8 o′ clock location of a counter clockwise rotating mill. Thus the action is taken to increase the mill sound up to a level beyond which it is considered that cataracting or direct ball strike on shell is taking place. In practice analysis of frequency peaks is made to discriminate between attrition and impact events. For this reason acoustic signal analysis is difficult and subjective at best. Most operations use sound level as a way of controlling mill speed and/or feed rate.

2.1.1.2.2 Force sensor

Force measurement is basically based on the determination of a displacement subject to loading. Strain gages have been primarily used to analyze forces but lately piezo-electric transducers are becoming more popular for the measurement of forces. In tumbling mills, the forces on the lifter bars are quite sensitive to impact and collision. Hence instrumented lifters incorporating force sensors have been used to monitor the performance of tumbling mills. These types of sensors are particularly useful to investigate the fluctuations in the load in SAG mills and identify extreme conditions that lead shutdowns.

2.1.2 Instrumented Sensor Package

The genesis of the instrumented grinding ball technology dates back to 1978, when David Dunn of Climax Molybdenum Company conceived of impact force measuring balls to evaluate stresses on mill liner materials. The objective then was to correlate measured impact stresses with service performance of mill liner alloys. With the express purpose of eliminating the need for miniature recording or transmitting electronic devices (and to survive impacts) David Dunn designed six spring type accelerometers. The central cavity in the grinding ball is made with a 3-inch nipple as shown in Figure 2.2. Figure 2.3 shows the two halves of a grinding ball fitted with three accelerometers in each half.

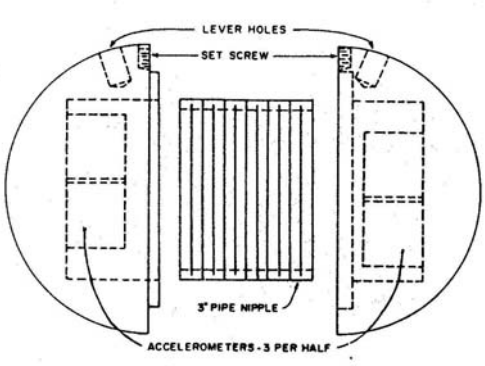

Figure 2.2 Central cavity and accelerometers.

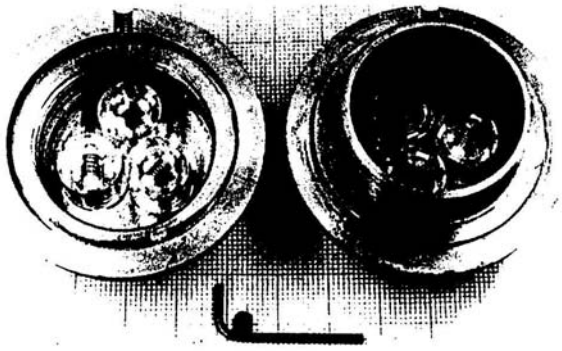

Figure 2.3 Grinding ball fitted with 3 accelerometers in each half.

The instrumented balls were recovered manually from mills. In an actual test in a 2.74m diameter mill operating at 72 tph the most severe impact was recorded at 200-250g. Based on the success of this test Dunn calculated forces and stress experienced by mills of different diameter (shown in Table 2.1).

Table 2.1 Grinding ball impact force and stress

Mill Diameter (m)	2.74	3.96	8.53
Mill Type	Grate discharge	Overflow	Semiautogenous
Mill Speed (rpm)	20	14.5	10.2
Ball drop height (m)	2.03	2.28	6.39
Impact deceleration (g's)	350	380	650
Impact Force (N)	62.3	6760	27,500 - 53,700
Impact Stress (MPa)	2200	2220	2980 - 3210

Dunn concluded that such testing in operating mills would lead to ways of protecting expensive and critical mill liners from the fatal stresses developed in mill operations.

Six years later, Rolf and Vonglukiet took the instrumented ball technology to a higher level. They installed a movable pestle, flush with the surface of the ball (as shown in Figure 2.4). The pestle is held in place by a spring. When an impact occurs, which exceeds the tension of the spring; the pestle is pushed in and activates an electric switch. This generates a counting pulse, which is recorded by a memory chip imbedded in the ball cavity. Upon retrieving the ball from the mill the data in the memory chip is transferred to a computer. By simultaneous use of instrumented balls with different tensions of the springs, they measured the distribution of impact energies in a 0.8 x 0.4 m mill with six instrumented balls. Figure 2.5 shows the impact energy spectra for different critical speeds of the mill. At 55% and 75% critical speed the impact frequencies are higher indicating optimum grinding regime (pulse) within the mill. At higher critical speeds (110% and 130%) the grinding pulse is greatly diminished due to centrifugation of the balls.

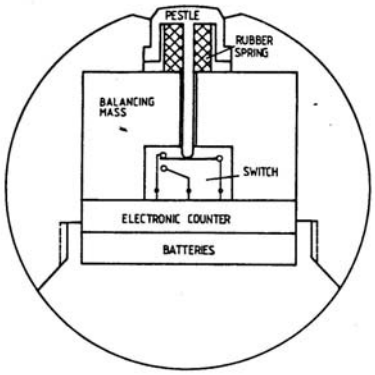

Figure 2.4 Movable pestle arrangement in grinding ball

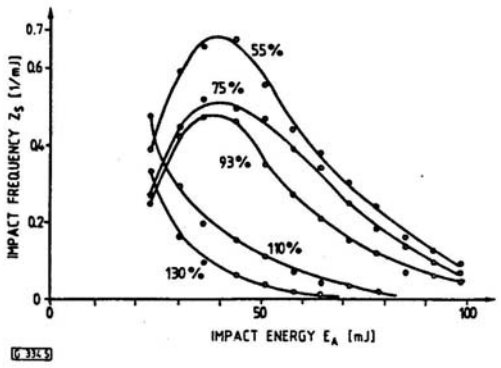

Figure 2.5 Impact energy spectra

Rajamani et al calculated the impact spectra of large diameter SAG mills using a numerical method known as the discrete element method. The software known as Millsoft predicted charge motion within the mill (Figures 4 and 5). The visualization of charge motion led to the development of shell lifter with a steeper face angle (22 to 30 degrees). Such lifters have been adopted by almost all mine sites around the world.

Millsoft software computes the impact energy spectra for a given set of conditions within the mill.

3. EXPERIMENTAL WORK ON A LAB SCALE MILL

3.1 Drop ball experiments

In a mill or a crusher, particles are stressed and broken by forces acting either on each particle directly or on a bed of particles. So to understand any size reduction process it is vital to understand the single breakage event, as size reduction is nothing but a cumulative process of these single breakage events over a longer period of time.

The loading and fracture of particles in tumbling mills occur within a very short period of time, about 150 microseconds for each individual breakage event. In an attempt to measure this kind of high-speed single particle breakage events, Ultra Fast Load Cell (UFLC) assembly was developed at the Utah Comminution Center. UFLC is a hybridization of conventional load cell, simple drop-weight apparatus and the Hopkinson Pressure bar. To understand the dynamics of single breakage event and to calibrate the new sensor package developed many drop-ball experiments were performed on the UFLC. A typical drop ball event has a force characteristic as described in Figure 3.1. The force of impact increases with time to a peak value which occurs just before the point of rebound from the surface. The curve then more or less retraces its path back to zero. The magnitude of the force is dependent on the ball mass and the drop height.

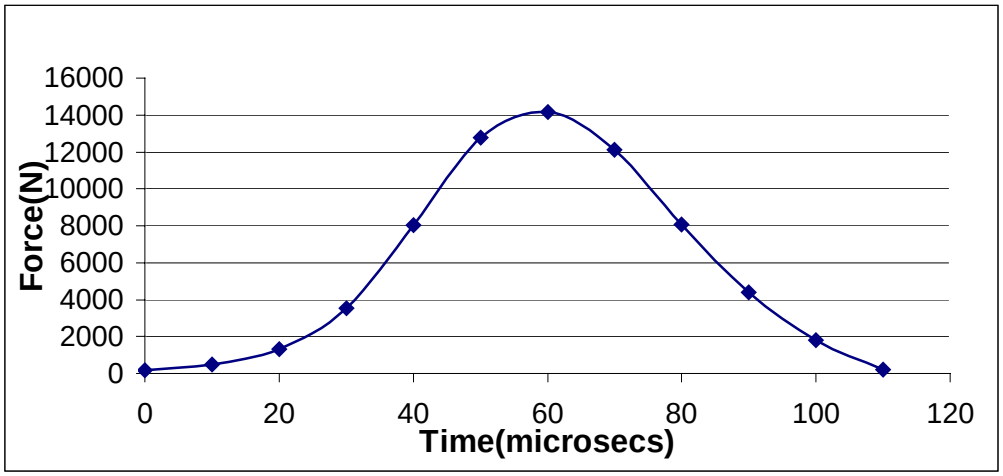

Figure 3.1 Force-time analysis for a steel ball of diameter 1.6 inch impacting from a height of 5 inches.

Figure 3.2 Ultra Fast Load Cell (UFLC)

To get a better understanding of the relation between impact force and time, more experiments were conducted changing the ball size and the drop height. It was found that impact force increases with both these variables as shown in Figure 3.3.

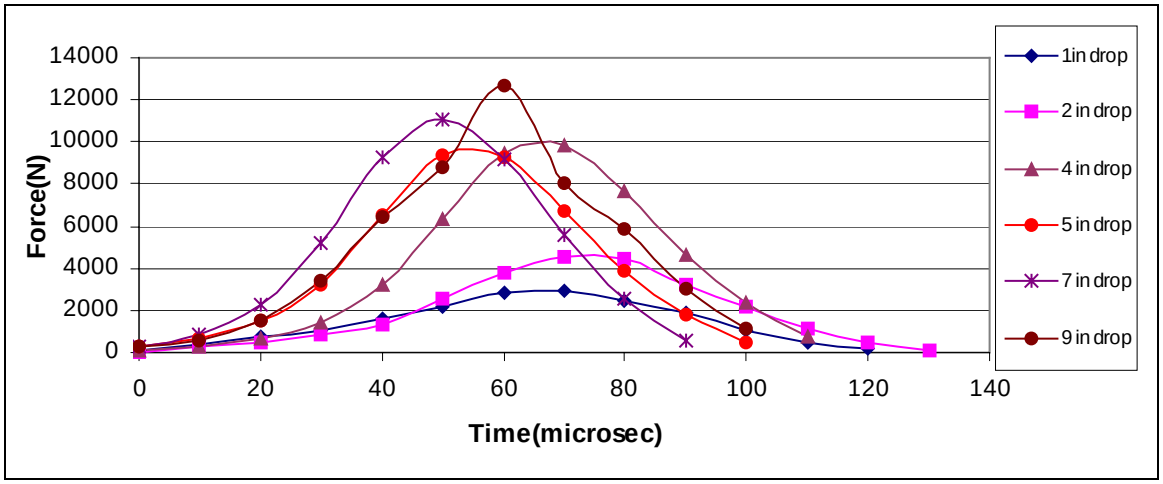

Figure 3.3. Force-time analysis for a steel ball of diameter 1.28 inch impacting from different heights

As can be concluded from the plot, the time for the rise and fall of force for each impact is about 100 to 150 microseconds. The peak force increases with increase in drop height. The ball size was changed to 1.6 inch and 2.16 inch to determine the effect of ball size on force profile.

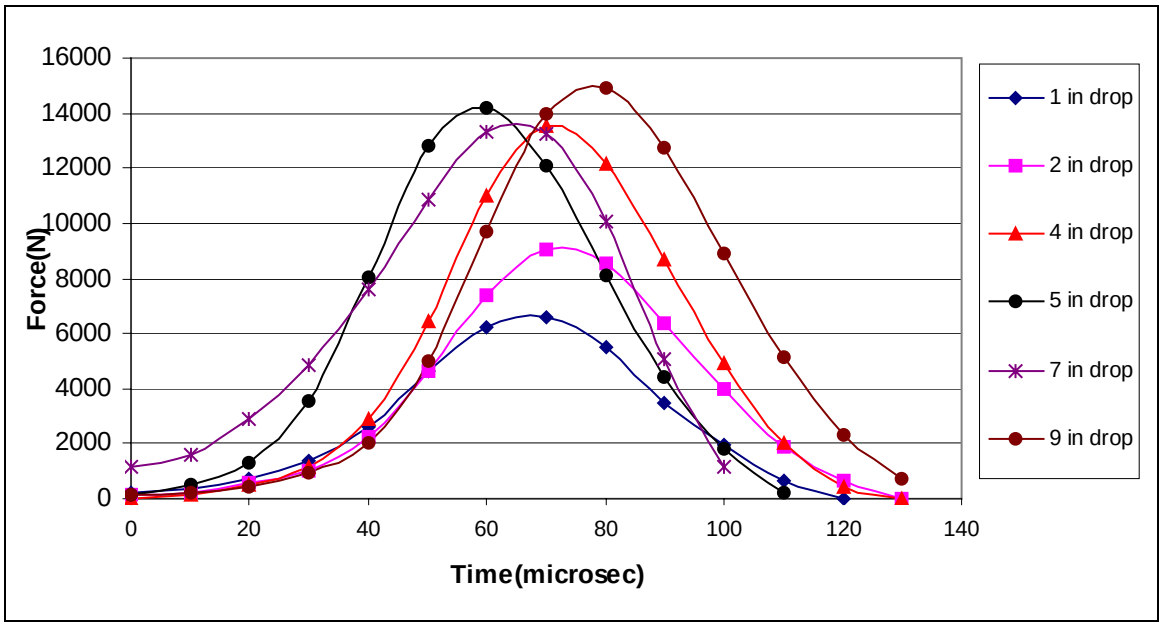

Figure 3.4 Force-time analysis for a steel ball of diameter 1.60 inch impacting from different heights.

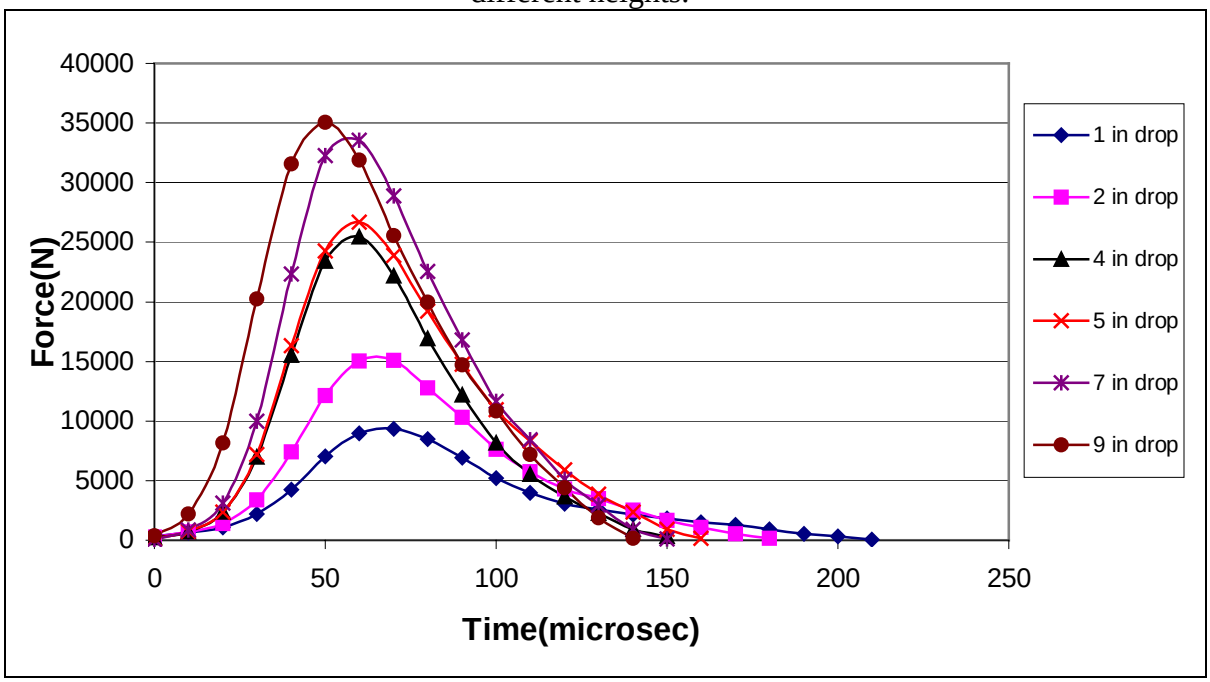

Figure 3.5 Force-time analysis for a steel ball of diameter 2.16 inch impacting from different heights

Figure 3.6 shows the plot of peak force experienced versus drop height for the three different ball sizes. It can be clearly seen in each plot above and from Figure 3.6 that

(i) For any particular ball, as the drop height increases the peak force increases.

(ii) For the same drop height, peak force increases as the ball size increases, i.e., as the ball mass increases.

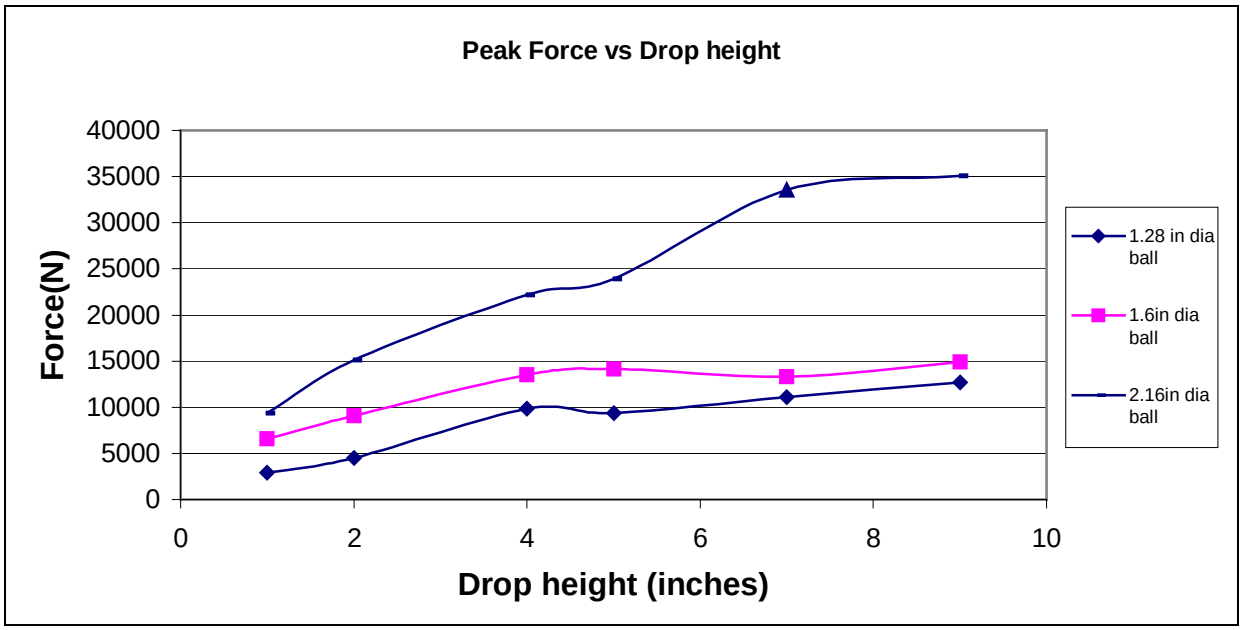

Figure 3.6. Peak Force vs. Drop height

From the above experiments, it was found that each breakage event occurs in small time intervals of 100 to 200 microseconds depending on the ball size and drop height. In order to record a breakage event, a data point has to be captured once at least every 10 microseconds. Hence, the main requirement for the load cell and the data logger assembly was that it had to record a sample data once in 10 microseconds, i.e. a sampling rate to of 10^5 samples/second.

3.2 Ball Mill Experiments

3.2.1 Experimental Set-up

The first stage of experiments was conducted in a laboratory scale ball mill. The ball mill measured 8.5 inches in diameter and 9 inches in length. The mill was run under dry conditions without any material in it. The experimental setup shown in the attached Figure 3.7 consists of a steel canister which runs on two rollers. As the rollers rotate, the ball mill placed on it also rotates. These rollers were powered by a variable speed motor.

The instrumentation required to capture the impact signals was attached to the mill on the back end. The load sensor package was welded to the inside of the ball mill as shown in Figure 3.8. The load cell used was made by Honeywell and had a range of 0-20000 lbs. There were two initial setbacks which had to be solved. The load cell had four output cables, two for power supply and two for signal which have to be connected to a read-out device. The power supply and the analog - digital board were both external to the mill. So a slip – ring was required to transfer the signals and power to and fro from the mill. The former problem was solved by running the wires parallel to the mill, safely protected in a half inch diameter steel pipe. A one inch hole was drilled though the back of the mill from which the steel pipe and the wires were brought out of the mill. The

latter problem was tackled by using a slip-ring contactor. A four pin slip-ring was screwed to a hollow steel pipe (slip ring holder) which was machined to exactly match the exterior dimensions of the slip ring. This slip ring holder was welded to the back of mill shell. The slip ring contactor was used to supply power to the amplifier which in turn supplied power to the load cell and, to transfer the signal from the amplifier. The in-line amplifier was also stuck to the mill for ease of operation. The amplifier supplied the power for the operation of the load cell. It also amplified the signal from the load cell to prevent attenuation.

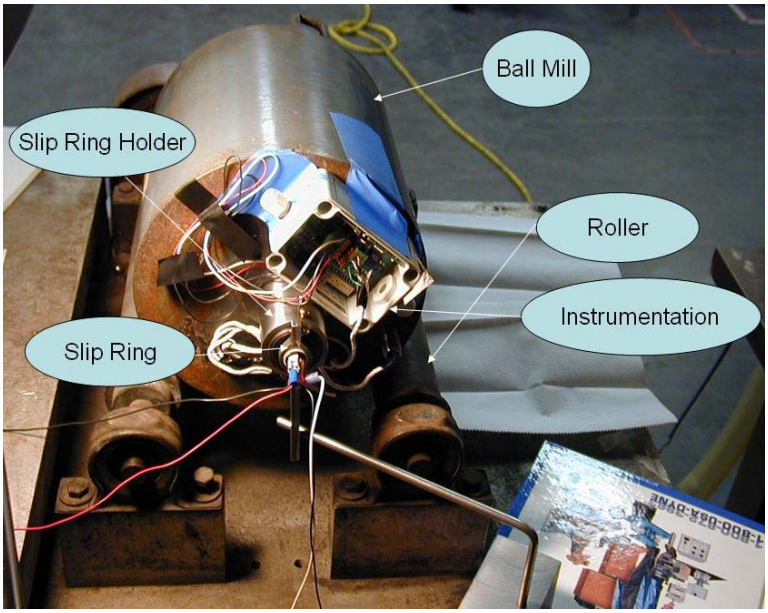

Figure 3.7 Ball mill with the instrumentation

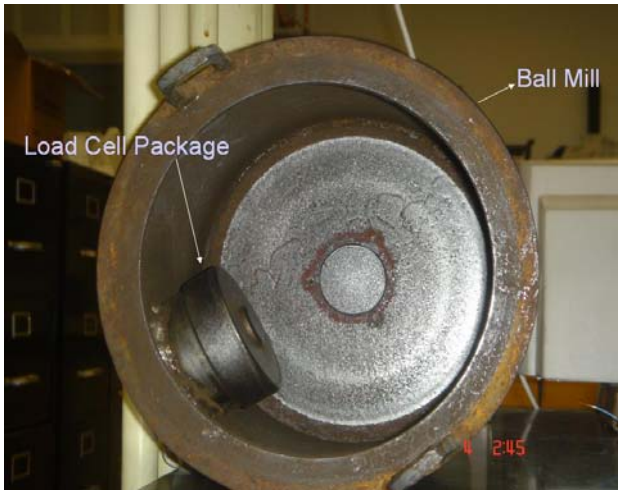

Figure 3.8 Load cell package welded to the mill

The load cell was packaged in a custom built steel cup holder and a cap. The load cell used was a button type load cell. The load cell package consisted of three parts - cup holder, cup cap and a floating cap as show in Figure 3.9.

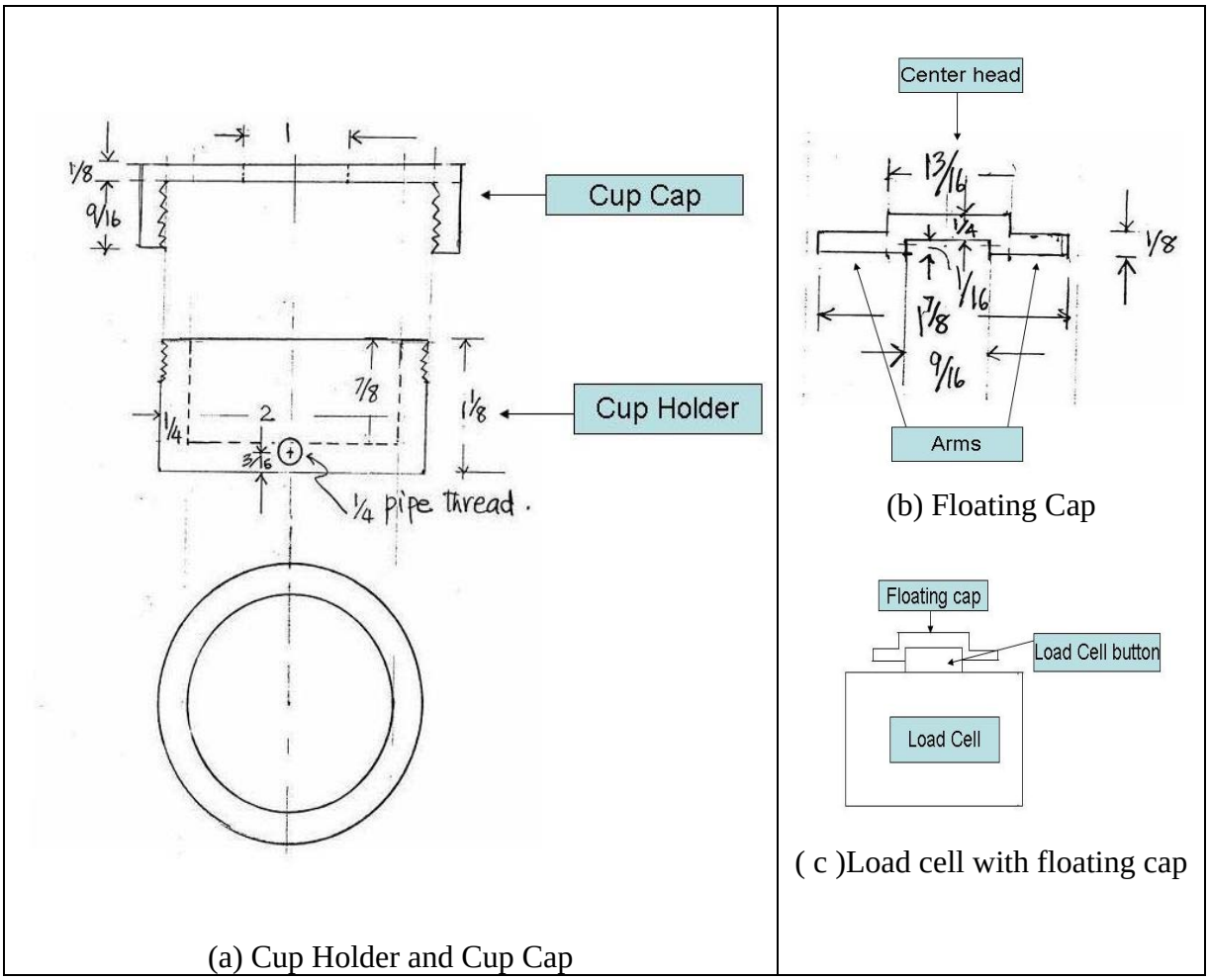

(a) Cup Holder and Cup Cap

(b) Floating Cap

(c)Load cell with floating cap

Figure 3.9 Design of load cell package

The floating cap was designed such that the center head would rest on the button of the load cell while the side arms float freely as shown is Figure 3.9 (c). The load cell was first placed in the cup holder. Then the floating cap was placed on the button of the load cell and it was tightened from the top using the cup cap. The head of the floating cap was exposed through the hole drilled on the cup cap. This way a hit on the head was directly transmitted to the button underneath. When there was an off-center hit the impact was transferred from the cup cap to the arm of the floating cap beneath it. It was then transferred to the button through the center head. Thus the assembly was designed to capture all the impacts, both on and off center.

The slip ring was attached to the mill using a slip ring holder. A slip ring holder is a hollow steel cylindrical shell custom made to the size of the slip ring as shown in Figure 3.10.

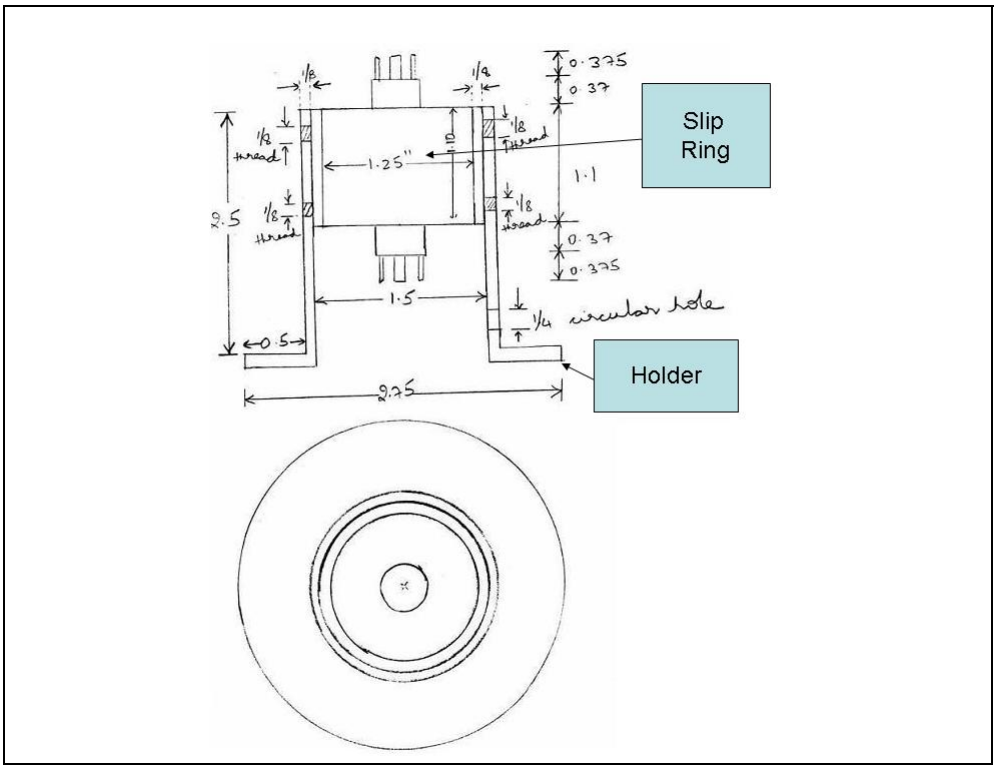

Figure 3.10 Slip Ring Holder

The slip ring holder was screwed to the mill shell so that it would not fall during rotation.

3.2.2 Test Conditions

The experiments in the lab mill were performed to investigate the relationship between the impact spectra and the operating conditions of the mill. The process variables used are listed in the Table 3.1. The tests were run without any material in dry state. The canister had no lifters attached to it. The main emphasis was to find out the sensitivity of the impact spectrum to change in the mill speed.

Table 3.1 Operating Variables Values

Design Variables	
Ball Size	1.27 inch, 1.11 inch
Mill Speed	60-80% critical speed
Mill filling	28%
Lifters	None

The first set of tests was conducted using 1.27 inch diameter steel balls at 28% mill filling. The mill speed was varied as 60%, 70% to 80% of critical speed. At each speed, the mill was run for 4, 8, 12, 16 and 20 minutes and the impact spectrum was collected. So, a total of 15 tests were performed using 1.27 inch steel balls. Later, the ball size was reduced from 1.27 inch to 1.1 inch and the mill was again run for 4, 8, 12, 16 and 20 minutes at 70% critical speed and 28% mill filling.

3.2.3 Experimental Procedure

1. The ball mill was filled with 1.27 inch steel balls at 28% filling and closed.
2. The speed of the mill was set at 60% critical speed.
3. The slip-ring contactor and the amplifier were connected carefully.
4. The signal output wires were then connected to the A/D converter which was in turn connected to the computer.
5. The mill was turned on.
6. The data acquisition button was switched on in the LabView program to collect the data and the time was noted simultaneously. This was marked as the start time.
7. LabView collected the data continuously for 4 minutes and was then turned off. The data was stored in a Microsoft Excel file for data analysis at a later stage.
8. The mill was then turned off.
9. Above steps 5 through 8 were performed changing the time of data collection to 8, 12, 16 and 20 minutes.
10. Each time the mill was stopped; all the connections were rechecked to ensure that they were right.
11. The mill speed was changed from 60% to 70% and then to 80% critical speed and the same steps as mentioned above were repeated.
12. Once the experiments with 1.27 inch balls were done, the ball size was changed to 1.1 inch. Here, the data was collected only at 70% critical speed as the relation between the impact spectra and the critical speed was already examined.
13. The processing of the data was done by running it through a MATLAB code which would identify the peak force corresponding to each impact and isolate it. It would also generate the impact spectra by identifying the number of impacts falling in a particular force range.
14. The impact spectra were then analyzed to identify the effect of the process variables.

The summary of the experimental conditions is given in the Table 3.2 below

Table 3.2 Experimental Conditions

Test ID	Ball Size(inch)	Mill Speed (%)	Time(minutes)
A-301	1.27	60	4
A-302	1.27	60	8
A-303	1.27	60	12
A-304	1.27	60	16
A-305	1.27	60	20
A-311	1.27	70	4
A-312	1.27	70	8
A-313	1.27	70	12
A-314	1.27	70	16
A-315	1.27	70	20
A-321	1.27	80	4
A-322	1.27	80	8
A-323	1.27	80	12
A-324	1.27	80	16
A-325	1.27	80	20

B-301	1.1	70	4
B-302	1.1	70	8
B-303	1.1	70	12
B-304	1.1	70	16
B-305	1.1	70	20

3.2.4 Results

After each experimental run, the data was analyzed to produce a force spectrum and a force histogram. The sample force spectrum and the sample force histogram are shown in Figures 3.11 and 3.12 respectively.

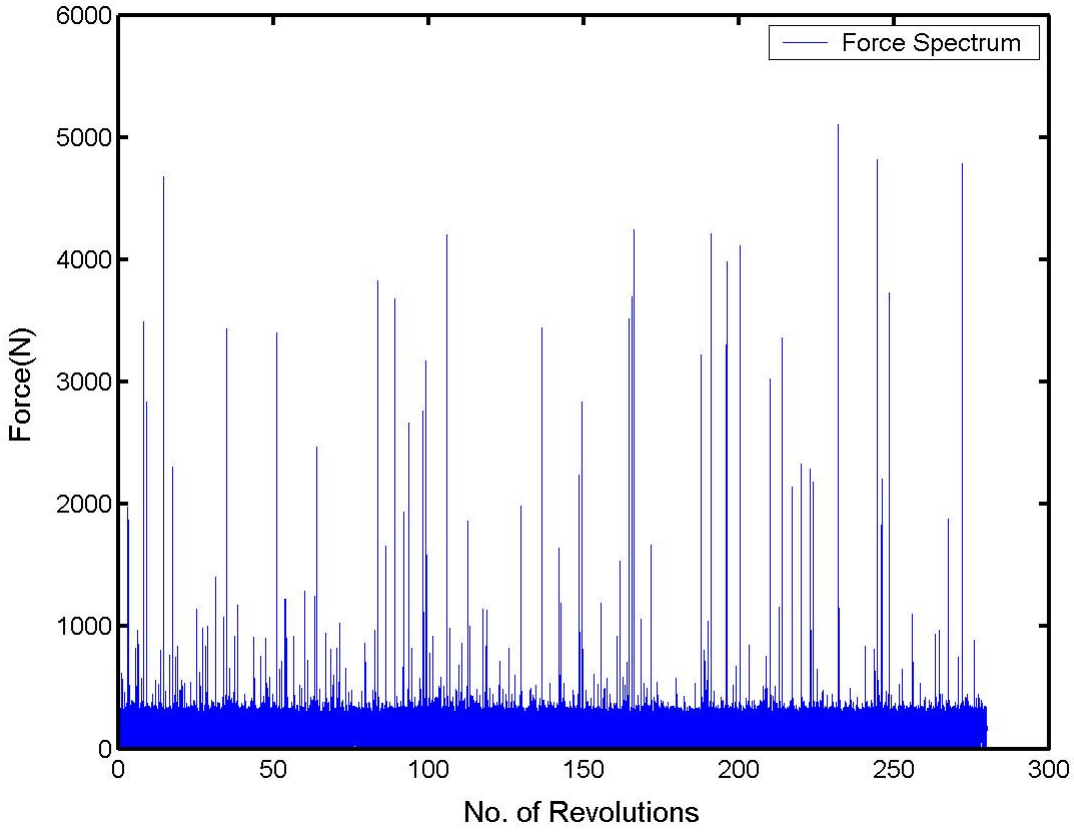

Figure 3.11 Sample Force Spectrum

A force spectrum is a plot of force in Newton versus the number of revolutions. It shows the rise and fall in the magnitude of the force corresponding to each impact. The variation in the peak forces can be seen conclusively in the above plot. It can be also seen that at any point of time, the number of smaller force impacts is much greater than the number of higher force impacts. By identifying the peak force corresponding to each impact and isolating it, force histogram was produced.

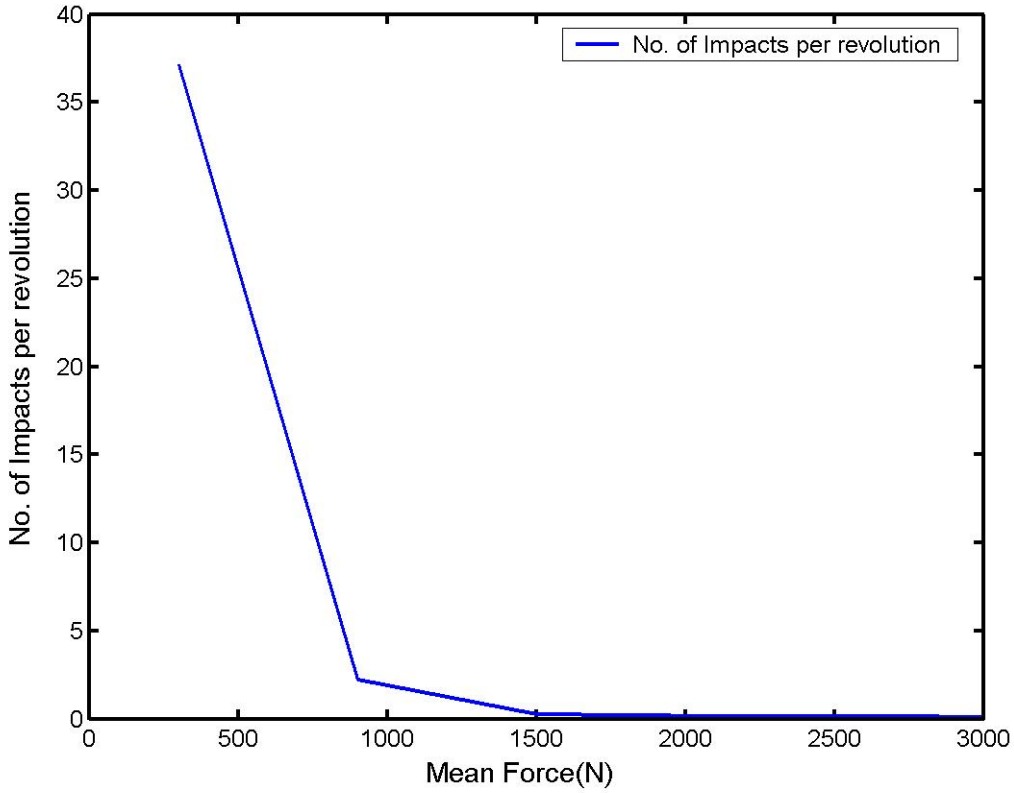

Figure 3.12 Sample Force Histogram

The force histogram is a plot of number of impacts per revolution on Y axis against the mean force in Newton. The force histogram can also be plotted as bar chart as shown in Figure 3.13. For better interpretation of the data the histogram is shown as two different plots. The force bins are divided into 10 equal bins from 0 N to 6000 N. Each bin is represented by the mean force of the bin i.e. the 0-600 N bin is represented by 300 N. The number of low force impacts is very high (>35) when compared to the number of high force impacts which are typically less than one. To see a clear trend in each bin, the histogram is divided into subplots.

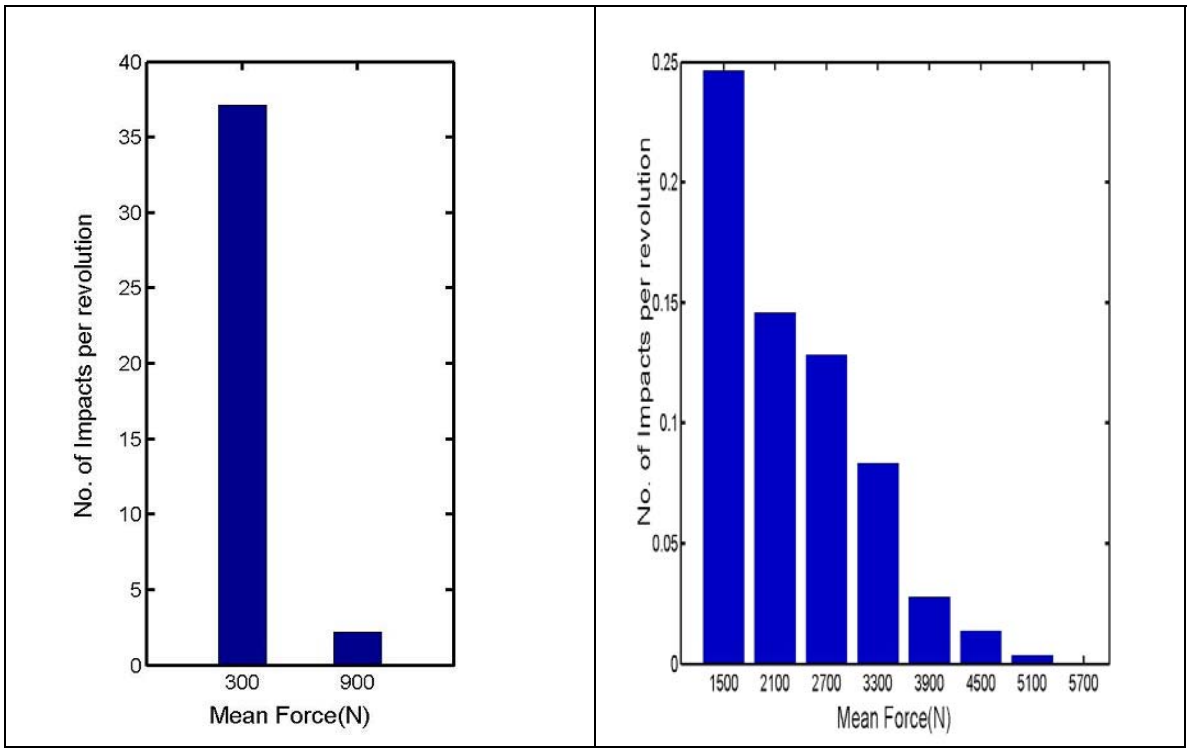

Figure 3.13 Number of impacts per revolution plotted against the mean force in N

3.2.4.1 Effect of Mill Speed

Figure 3.14 shows the impact spectra collected at 80% critical speed using 1.27 inch steel balls. It shows the data corresponding to the five different run times and the average of the five runs.

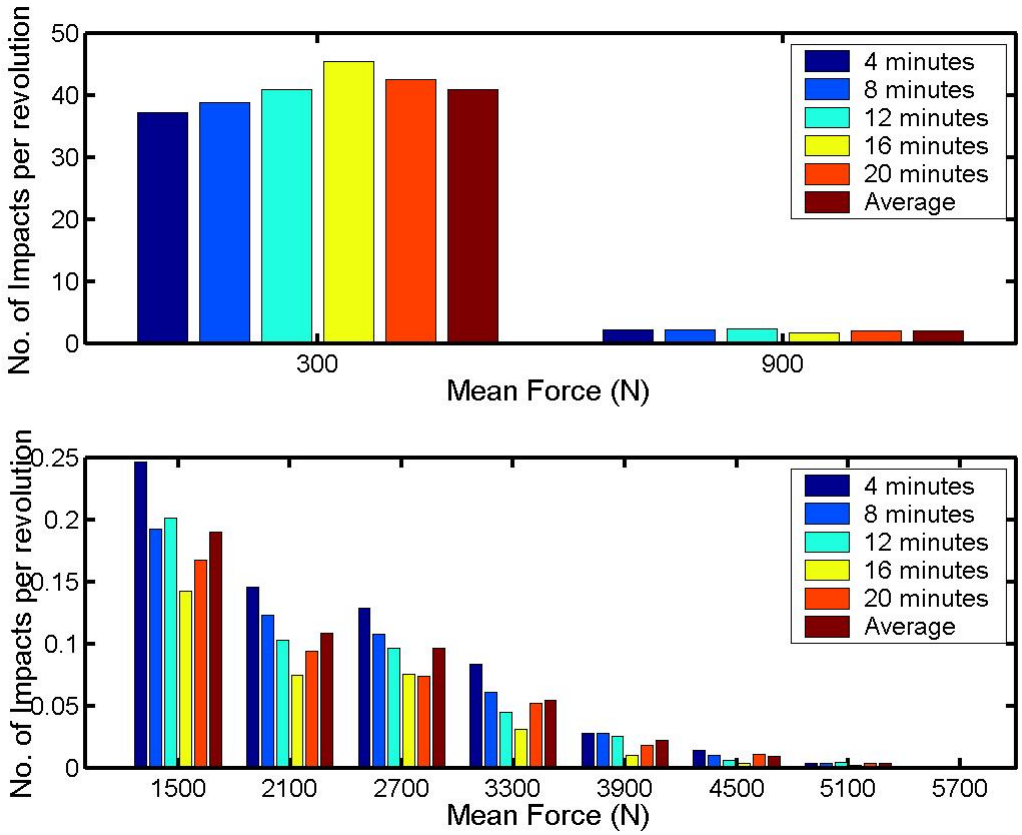

Figure 3.14 Impact Spectra at 80% critical speed

The following conclusions can be drawn form Figure 3.14. The number of impacts per revolution at different run times is nearly the same. The collected impact spectra are unchanging beyond 4 minutes and hence the data collected for five minutes can be treated as a good representation of the impact spectrum. There is a sharp decrease in the number of impacts per revolution from the first bin to the second bin and from there on for each bin there is a progressive decrease. It has been clearly observed that in the lower force ranges, the number of impacts decrease with the increase in critical speed. This can be seen in Figure 3.15 below.

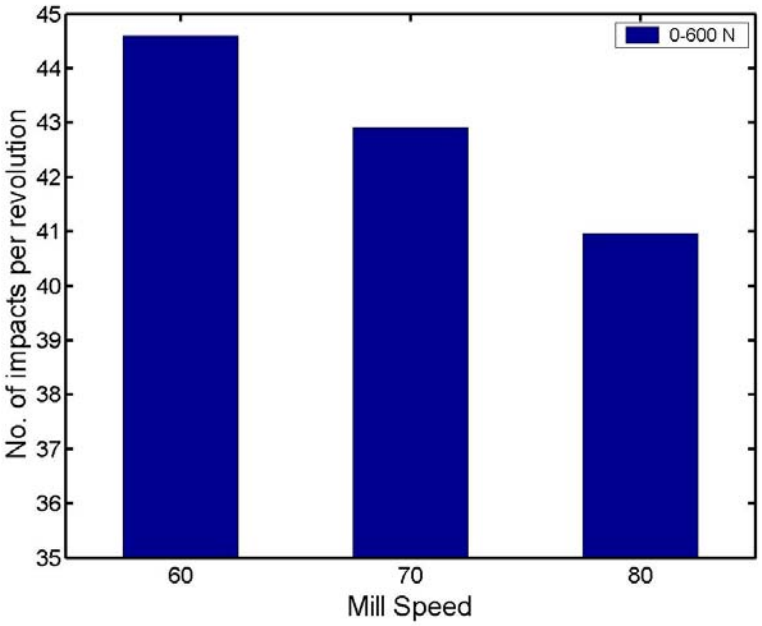

Figure 3.15 Impacts per revolution in the 0-600 N force range at each mill speed

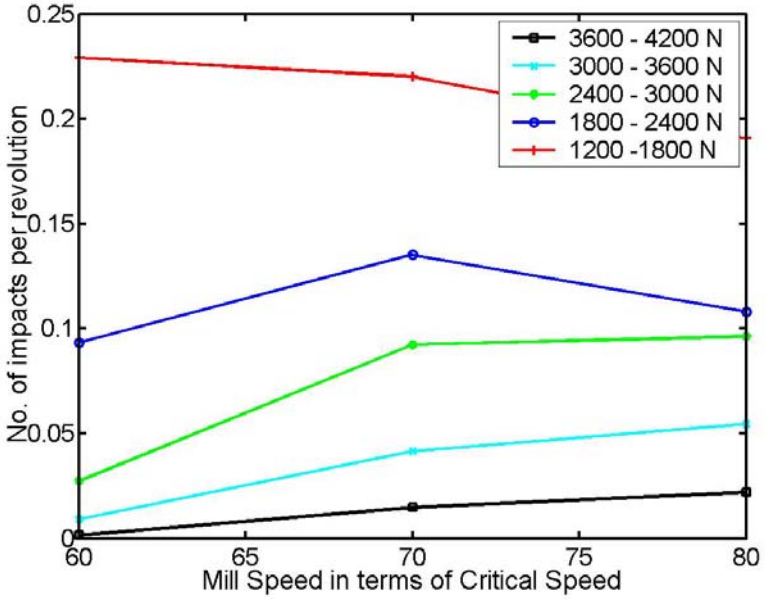

Figure 3.16 Impacts in different force ranges per revolution versus mill speed

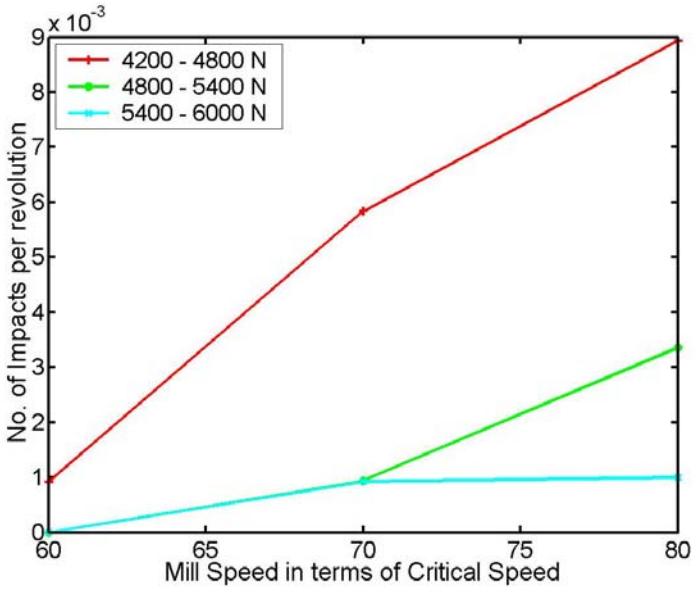

Figure 3.17 Impacts in different force ranges per revolution versus mill speed

It can be observed from Figures 3.15, 3.16 and 3.17 that as the force range is increased, the graph gradually shifts from a decreasing trend to an increasing trend. This trend is magnified in the force range 4200-4800 N seen in Figure 3.18.

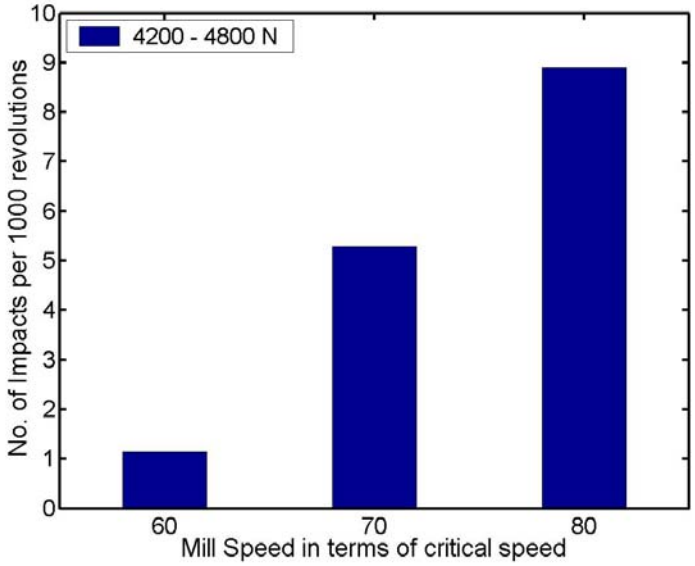

Figure 3.18 Impacts per 1000 revolutions 4200 – 4800 N bin versus mill speed

In lower force ranges (till about 1200 -1800 N), the number of impacts per revolution decrease as the critical speed increases. In the higher force ranges (2400 - 3600 N and higher), the number of impacts per revolution increase with an increase in the critical speed. For the force range 1800 – 2400 N, the trend is neither increasing nor decreasing. It increases from 60 to 70% critical speed and decreases from 70 to 80% critical speed. As the mill speed increases, the charge motion slowly shifts from

cascading to cataracting and cataracting implies high force impacts. Thus, the result obtained above agrees with the theory that as we move closer to the critical speed, the number of low force impacts would decrease and the number of impacts with higher force would increase. The impact spectra generated at 70% critical speed and 60% critical speed are also similar to the above figure and can be found in the appendix.

3.2.4.2 Effect of Ball Size

To determine the effect of ball size on the impact spectra, the impact spectrum generated at 70 % critical speed using 1.27 inch ball was compared with impact spectrum generated using 1.1inch balls under same operating conditions. The results are shown in the Figure 3.19 and 3.20.

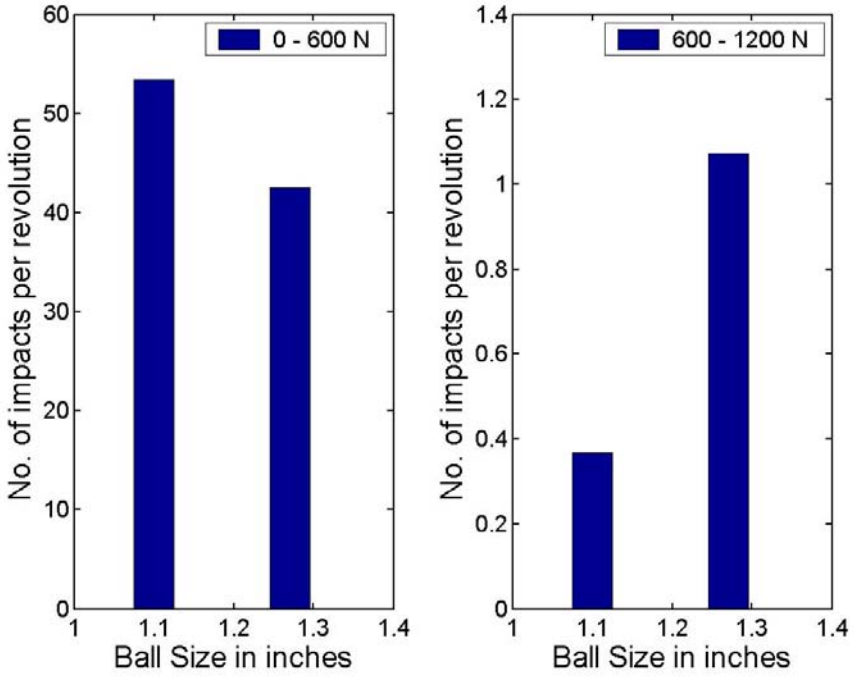

Figure 3.19 Number of impacts per revolution versus ball size

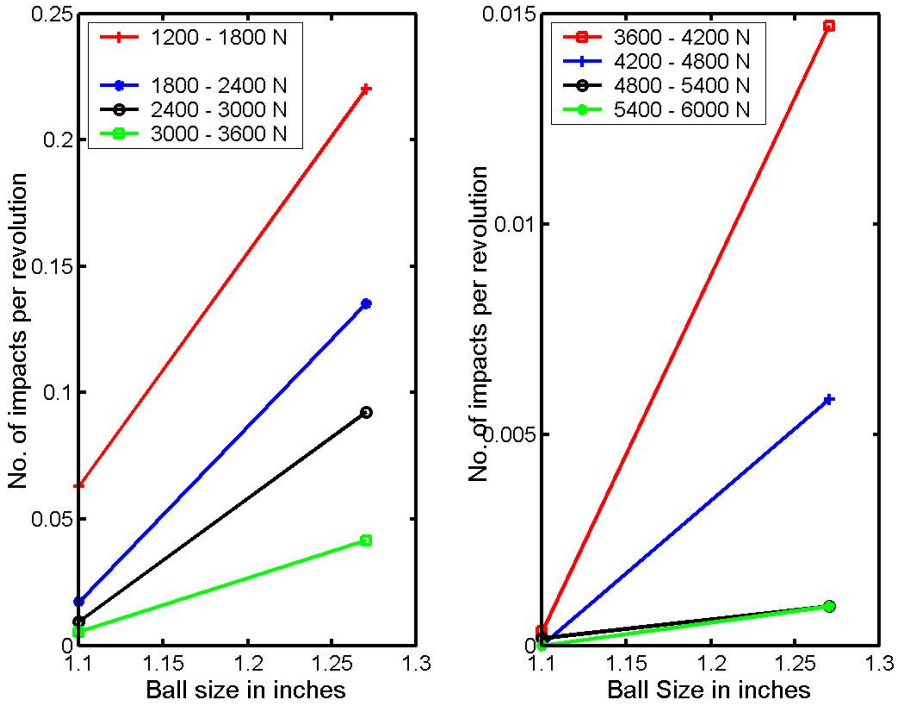

Figure 3.20 Number of impacts in different force ranges per revolution versus ball size

In the small force range 0-600 N, the number of impacts per revolution is higher using 1.1 inch balls than the 1.27 inch balls. This trend is however reversed as the force range increased. As the ball size increases, the ball mass also increases. So, the force of impact for the same drop height increases which leads to an increase in the number of impacts in each force bin except the first one.

4 EXPERIMENTS ON THE PILOT SCALE MILL

4.1 Experiments in pilot mill

4.1.1 Experiment Set-up

Experimental studies were conducted on the existing pilot ball-mill set-up shown in **Error! Reference source not found.**. The load cell design was the same as used for the ball mill. A few minor changes were made to adapt it to survive the pilot mill conditions. The mill was run in dry conditions without any material. The first set of experiments was conducted to get a general idea of the nature of impact spectrum and the kind of forces acting in the mill.

4.1.1.1 Pilot mill design

The pilot-scale mill was a cylindrical steel shell measuring 0.416 m in diameter, 0.641 m in length and 18 mm in thickness. On the cylindrical shell there was a

rectangular opening of 178 mm by 127 mm through which grinding balls were introduced or removed. The feed end was a steel plate with a 51 mm diameter hole at the center to which a drum feeder was attached. A screw feeder 3 m long and 0.127 m diameter was used to transport ore from the bin to the drum feeder. The discharge end consisted of a grate plate. The grate plate was made up of 6 mm grate holes drilled in 5 concentric circles. The circles were respectively 80, 80, 64, 64 and 48 mm in diameter. Two roller bearings were installed on the mill frame one near the discharge end and the other at the feed end to support the mill. The mill was fitted with eight rectangular shell liners. The liners measured 620 mm in length, 30 mm in width and 20 mm in height. Three central threaded screws held the lifter on the shell.

A torque sensor between the motor and the gearbox measured the torque at the drive side of the gear box. The torque signal was displayed on a digital indicator. A triangular frame supported the mill assembly. A Rice Lake ^{TM} weighing system, which included three paramount ^{TM} load sensors were anchored to the supporting concrete block. Hence, the triangular frame rests on the load sensors. The pilot mill is shown in Figure 4.1

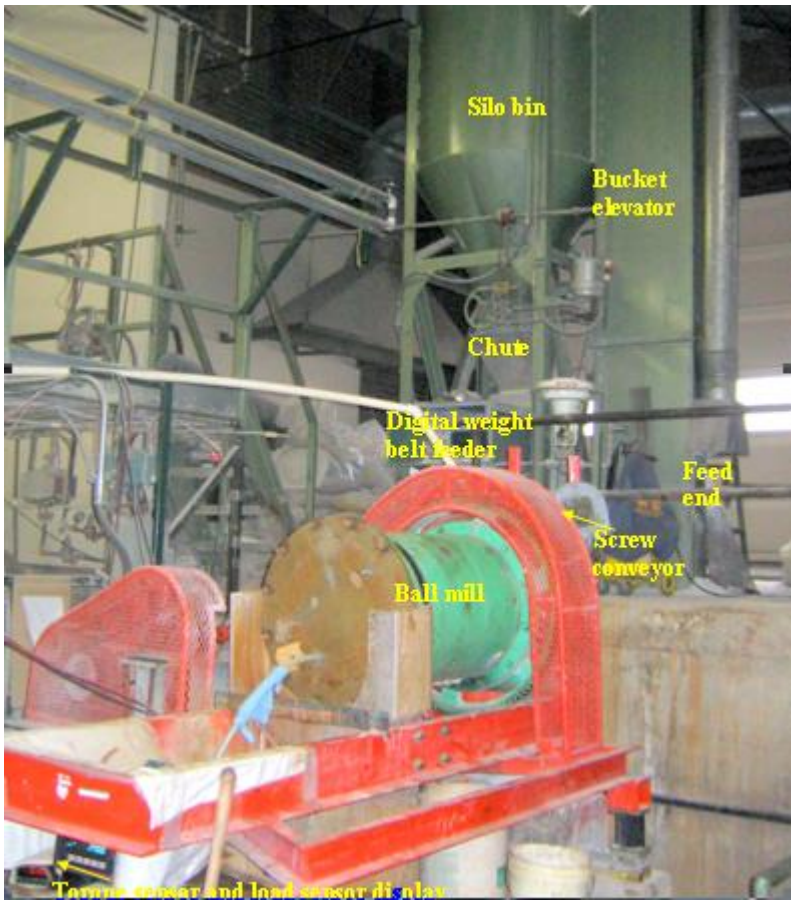

Figure 4.1 Pilot scale ball mill

4.1.1.2 Load cell package design

The load cell package design was the same as used for lab scale ball mill experiments. The load cell used was 20000 lbs range bonded foil strain gauge transducer

manufactured by Honeywell Sensotec. It was specifically engineered for compression force measurements. It had an integral load button machined as part of the design.

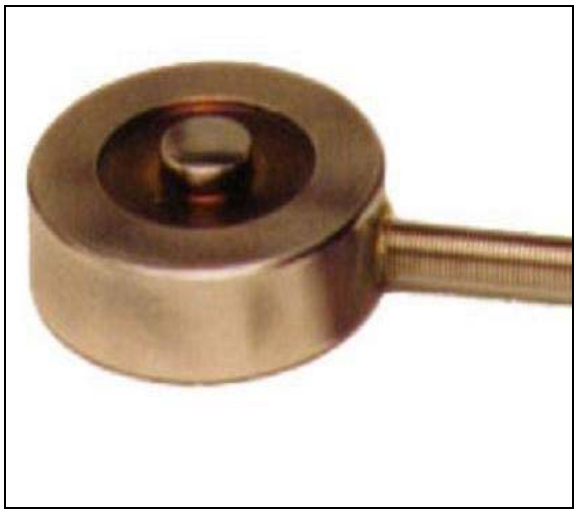

Figure 4.2 20000lbs range miniature load cell manufactured by Honeywell Sensotec

The load cell was of sub miniature kind measuring only 2 inch in diameter and 1 inch in height. This relative small size for a sensor with 20000 lbs range gave the flexibility of attaching it to the lifter inside the mill shell. The load cell was jacketed in the same load cell holder used earlier for ball mill experiments. The same load cell cap and the same concept of floating cap concept were used here again. The load cell package is shown in Figure 4.3

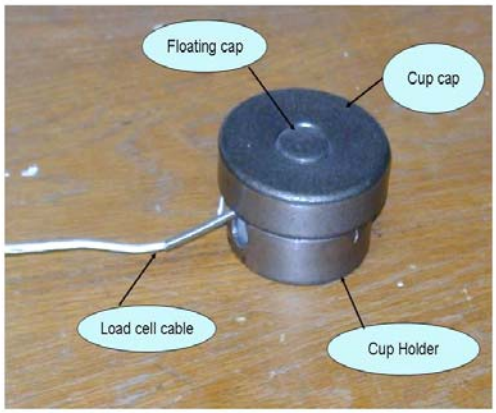

(a) With cup cap

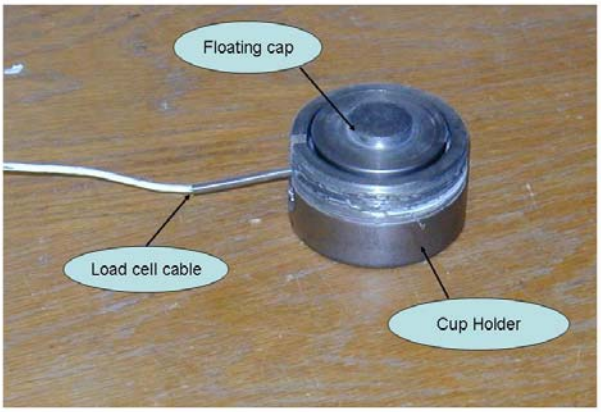

(b) Without cup cap

Figure 4.3 Load cell package

4.1.1.3 Load cell package attached to the mill shell

The load cell package was attached to the lifter inside the mill. A 2.5 inch x 0.375 inch groove was cut on the lifter to provide room for the load cell package as shown in Figure 4.5. Figure 4.4 shows the true dimensions of an uncut lifter.

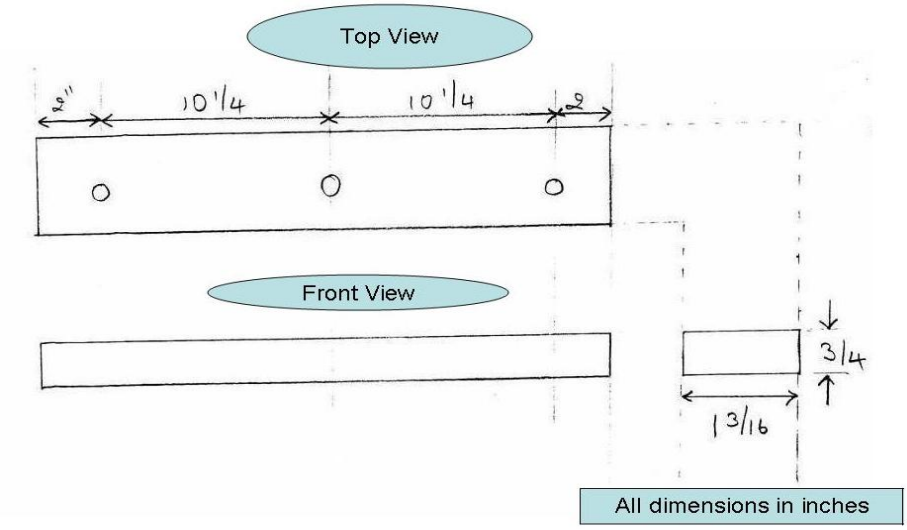

Figure 4.4 True dimensions of a lifter

Three holes were drilled on the load cell package to hold it against the lifter. Corresponding holes were drilled on the lifter (shown in Figure 4.6). A 0.5 inch diameter steel pipe was made to protect the load cell cables. This pipe was made to run parallel to the lifter. It ran from the center of the lifter where the load cell package was attached to the discharge end of the mill as shown in Figure 4.7. On the grate plate a 0.5 inch hole was drilled corresponding to the position of the pipe. The pipe was brought out of the mill through this hole.

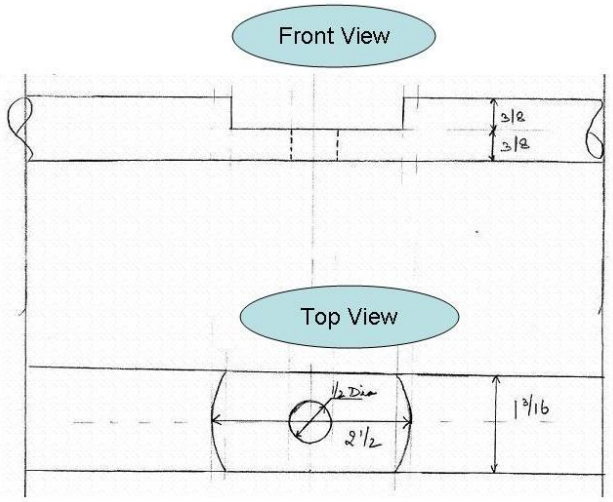

Figure 4.5 Font and top views of a lifter with a groove cut for the load cell package

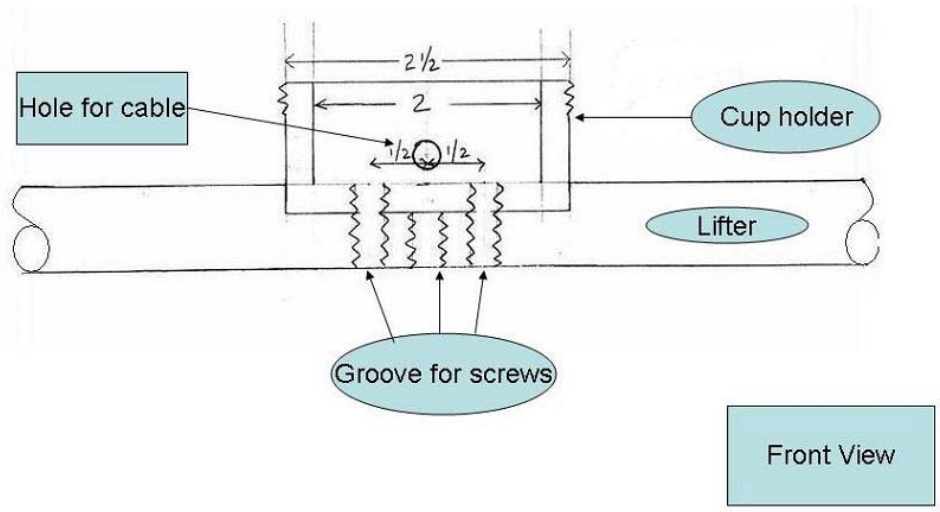

Figure 4. 6 Load cell package to the lifter bar

The slip ring, slip ring holder and the in-line amplifier were attached to the grate plate. The cables passing to the grate plate end of the mill through the pipe were connected to the amplifier to prevent the attenuation of the signal. The input power to the amplifier and the output signal from the amplifier was passed though the slip ring. The amplifier in turn powered the load cell and collected the output signal from the load cell. Data acquisition software, LabView was used to collect the raw data. Figure 4.8 shows the instrumentation attached to the grate plate of the mill.

Figure 4.7 Load cell package attached to lifter

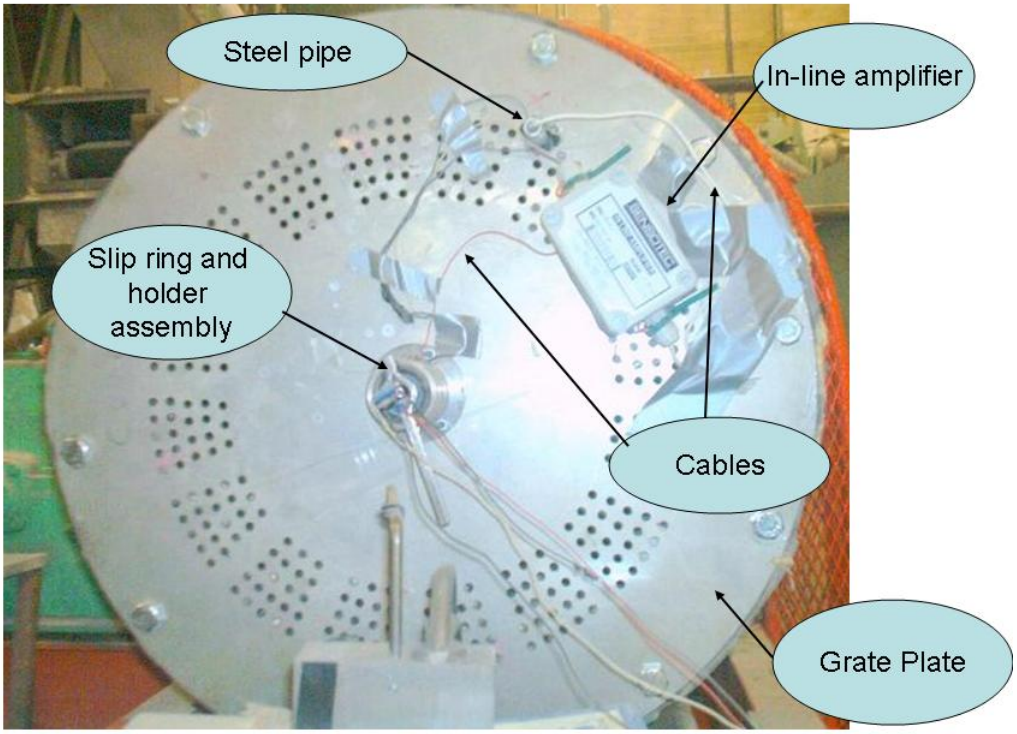

Figure 4.8 Instrumentation attached to the grate plate

4.1.2 Test Conditions

The main focus of these experiments was to determine the general magnitude of forces acting in the pilot mill and to check if the impact spectra were varying with operating mill parameters. For this purpose only the mill speed was varied and the impact spectrum showed an excellent correlation to mill speed. Table 4.1 shows the mill operating parameters. The mill was run in a dry condition without any feed.

Table 4.1 Mill operating parameters

Process Variables	
Mill Speed	60% to 95% in increments of 5%
Mill Filling	15% by volume
Critical Speed of mill	62 rpm
Time of operation	5 minutes

A mixture of different size of steel balls was used as charge. The size distribution of steel balls used is presented in Table 4.2

Table 4.2 Size distribution of charge used

Size (mm)	Number used
19.79	145
15.8	17
13.365	205

9.7386	213
6.822	77

4.1.3 Experimental Procedure

1 The mill was filled with steel balls up to 15% mill volume and closed.
2 The speed of the mill was set at 60% of the critical speed.
3 The slip-ring contactor and the amplifier were connected carefully.
4 The signal output wires were then connected to the A/D converter which was in turn was connected to the computer.
5 The mill was turned on.
6 The data acquisition button was switched on in the LabView program to collect the data and the time was noted simultaneously. This was marked as the start time.
7 LabView collected the data continuously for 5 minutes and was then turned off. The data was stored in a Microsoft Excel file for data analysis at a later stage.
8 The mill was then turned off.
9 The mill speed was changed in increments of 5% till 95% of the critical speed and the steps 5 through 8 were repeated each time.
10 Each time the mill was stopped all the connections were rechecked to ensure that they were right.
11 The processing of the data was done by running it through a MATLAB code which would identify the peak force corresponding to each impact and isolate it. The code would also generate the impact spectra by identifying the number of impacts falling in a particular force range.
12 The impact spectra were then analyzed to identify the effect of mill speed.

The summary of the experimental conditions is given in Table 4.3:

Table 4.3 Experimental Conditions

Test ID	Mill Speed (% critical speed)
A-401	60
A-402	65
A-403	70
A-404	75
A-405	80
A-406	85
A-407	90
A-408	95

4.1.4 Results

The impact spectra clearly moved with a change in the mill speed. The results matched with the prediction to a very good extent. The impact spectra results are presented in Table 4.4.

Table 4.4 Impacts spectra distribution

Force Range (N)	Mill speed as percentage of critical speed							
	60%	65%	70%	75%	80%	85%	90%	95%
0-250	88	95	48	47	46	44	49	49
250-500	31	30	19	20	19	17	18	16

500-1000	0.89	1.0	0.89	1.1	0.85	0.72	0.60	0.39
1000-2000	0.06	0.05	0.12	0.12	0.12	0.05	0.07	0.04
2000-3000	0.01	0.02	0.08	0.05	0.02	0.01	0.02	0.01
3000-5000	0.01	0.01	0.07	0.04	0.01	0.04	0.01	0.01
5000-7000	0	0	0.02	001	0.01	0.01	0	0
7000-10000	0	0	0.02	0.01	0	0.01	0.01	0
10000-12000	0	0	0.01	0	0	0	0	0
12000-15000	0	0	0	0	0.01	0	0	0

Graphical representation of this data is shown in Figure 4.9

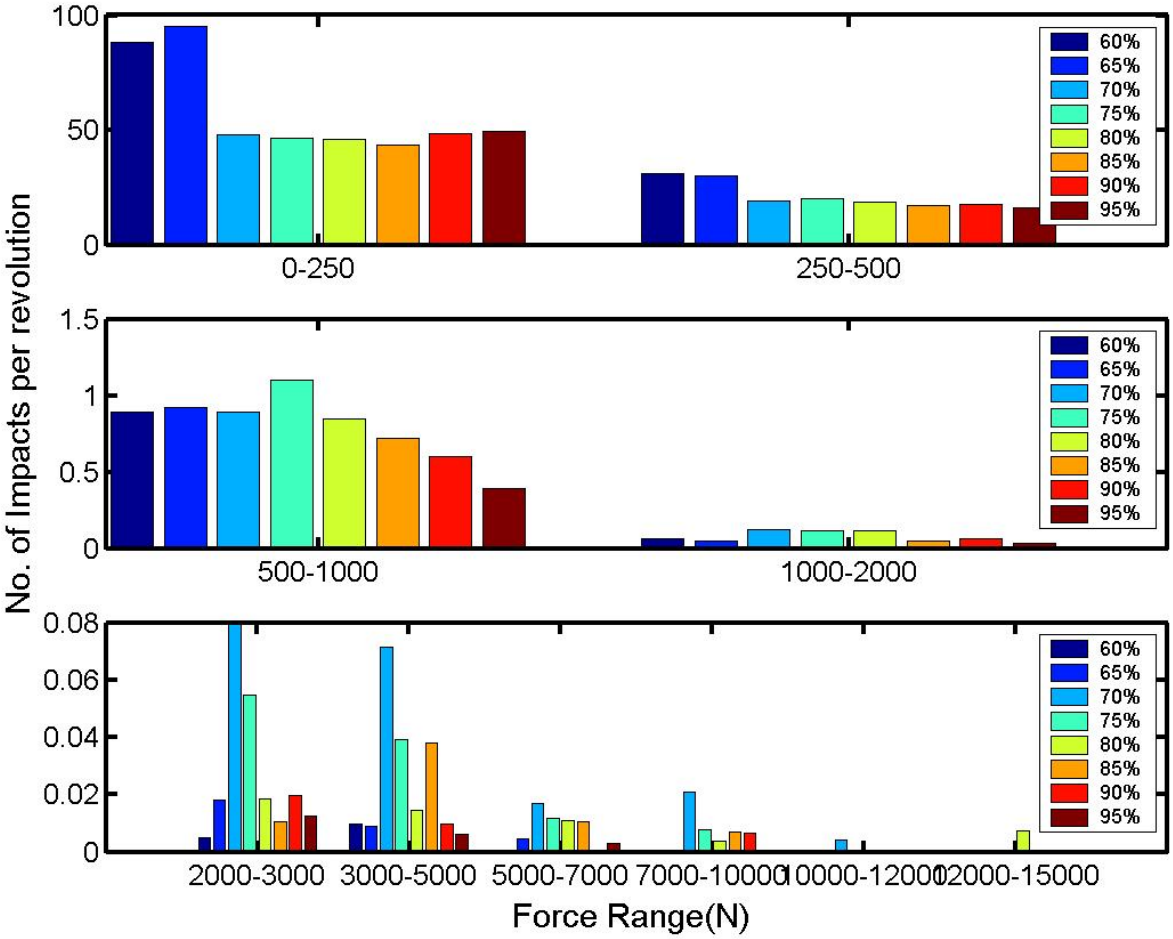

Figure 4.9 Comparison of Impact Spectra with force ranges at different mill speeds

In the above plot it can be seen that in smaller force ranges 0-250 N and 250-500 N, the number of impacts per revolution are about constant at 60% and 65% critical speed and decrease significantly from 65% to 70%. This is the point about which the charge shifts from cascading motion to cataracting motion. They are again about constant from 70% to 95%. As the speed of the mill increases, the ball starts to undergo cataracting

motion inside the mill. This leads to the balls dropping from a higher elevation to the toe and producing higher force impacts. For same reason, the number of impacts in higher force ranges (500-1000 N and beyond) is always maximum at 70%, 75% or 80% critical speed. At extremely high speeds of 90% and 95% critical speed, the steels balls begin to centrifuge to the mill shell leading to low overall number of impacts.

5 FINAL REVISION TO INTEGRATED LOAD SENSOR PACKAGE

5.1 Final Pilot mill Experiments

5.1.1 Experimental Set-up

The pilot mill used for the experiments was the 0.42 x 0.64 m mill used in earlier experiments. However, the load cell design was substantially changed. A further revision of the load cell package was used for more accurate and precise data. Several experiments were performed to determine the effect of mill speed, mill filling and ball size on the impact spectra. Promising results were obtained during the process.

5.1.1.1 Pilot Mill design

The pilot-scale mill is a cylindrical steel shell measuring 0.416 m in diameter, 0.641 m in length and 18 mm in thickness. On the cylindrical shell there was a rectangular opening of 178 mm by 127 mm through which grinding balls were introduced or removed. The feed end was a steel plate with a 51 mm diameter hole at the center to which a drum feeder is attached. A screw feeder 3 m long and 0.127 m diameter was used to transport ore from the bin to the drum feeder. The discharge end consisted of a grate plate. The grate plate was made up of 6 mm grate holes drilled in 5 concentric circles. The circles were respectively 80, 80, 64, 64 and 48 mm in diameter. Two roller bearings were installed on the mill frame one near the discharge end and the other at the feed end to support the mill. The mill was fitted with eight rectangular shell liners. The liners measured 620 mm in length, 30 mm in width and 20 mm in height as shown in Figure 5.2. Three central threaded screws held the lifter on the shell. The pilot mill is shown in Figure 5.1

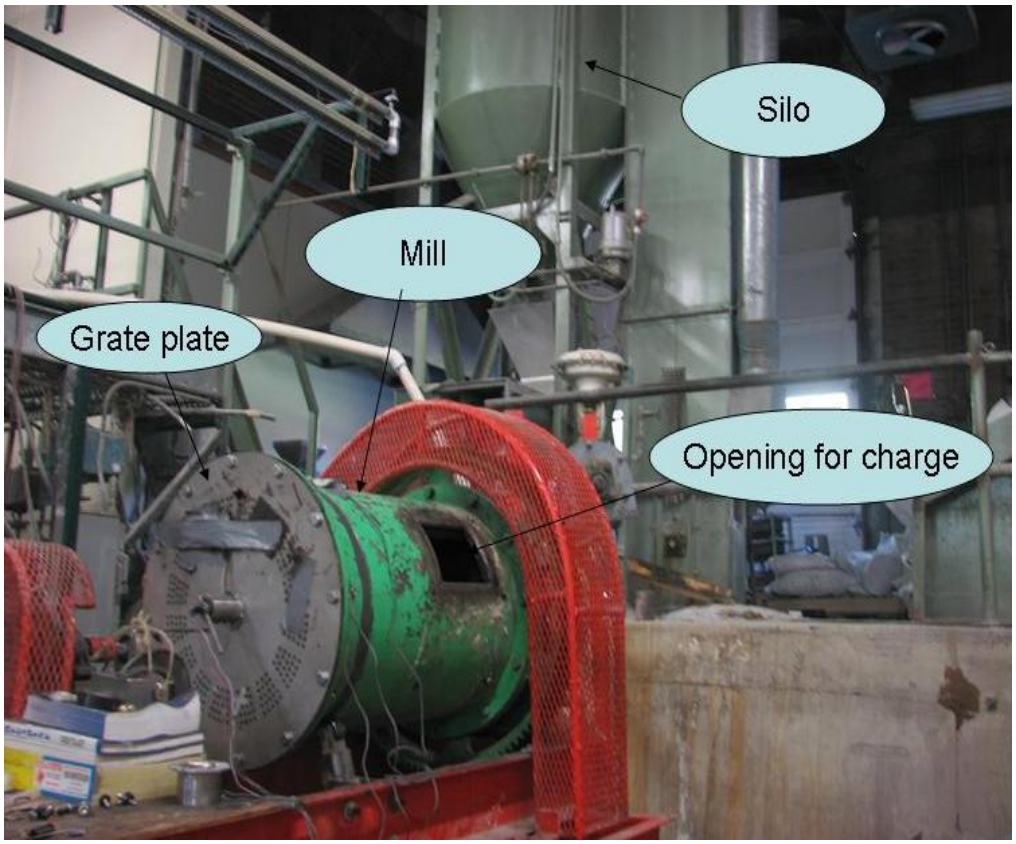

Figure 5.1 Pilot scale ball mill

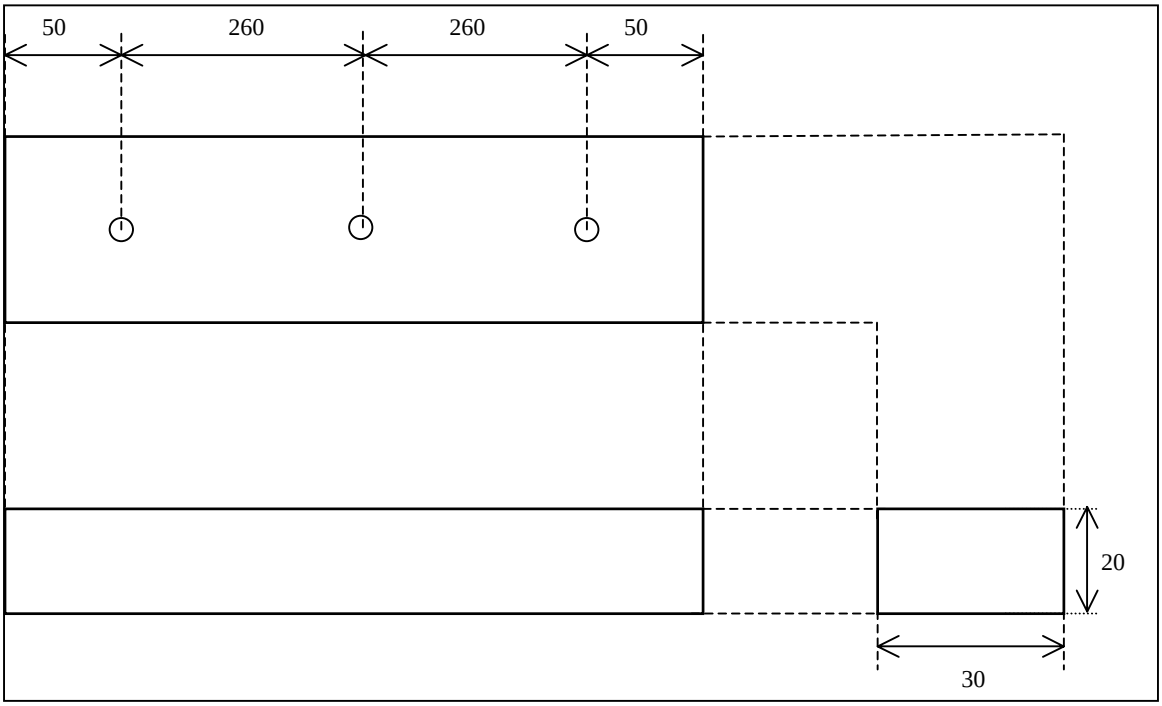

Figure 5.2 Shell lifter (dimensions in mm)

5.1.1.2 Load Cell Package Design

The load cell package consisted of a 5000 lbs load cell, manufactured by Transducer Techniques, enclosed in a stainless steel jacket. The load cell was a SSM series stud type load cell which could be surface mounted. It had eight thread mounting holes provided on the bottom surface for fastening. The sensing element was a bonded foil strain gauge to provide the highest quality resolution. The load cell was pressure sealed for protection from the environment which made it rugged enough to be used in a ball mill.

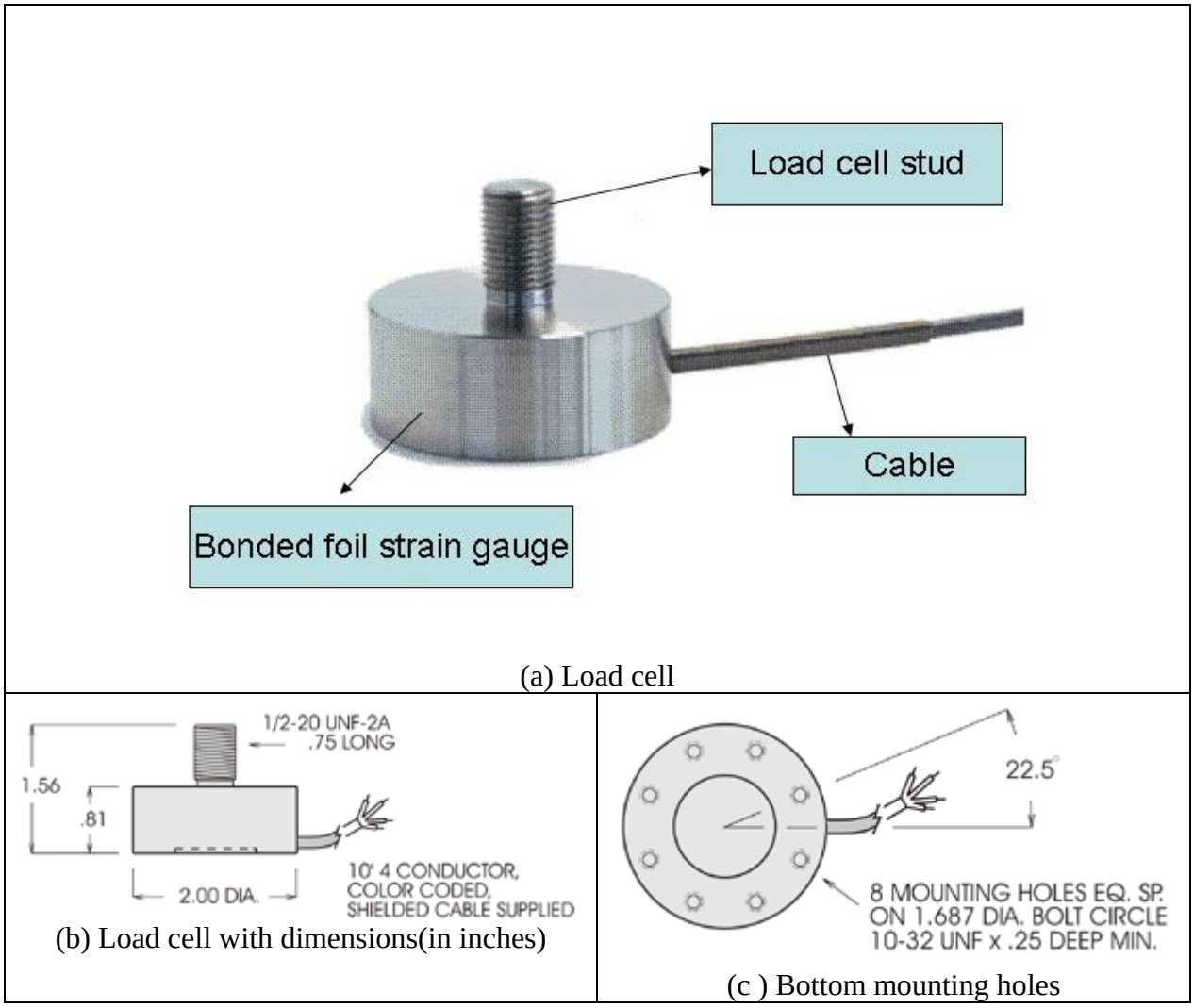

(a) Load cell

(b) Load cell with dimensions(in inches)

(c) Bottom mounting holes

Figure 5.3 5000 lbs load cell made by Transducer Techniques (SSM series)

The steel jacket surrounding the load cell was custom made to perfectly snug the load cell on all sides. The jacket consisted of three parts (a) the cup holder (b) the cap and (c) the stud. The cup holder had eight holes threaded on it corresponding to the holes on the load cell. Figures 5.4, 5.5 and 5.6 show the cup holder, cup cap and the stud respectively.

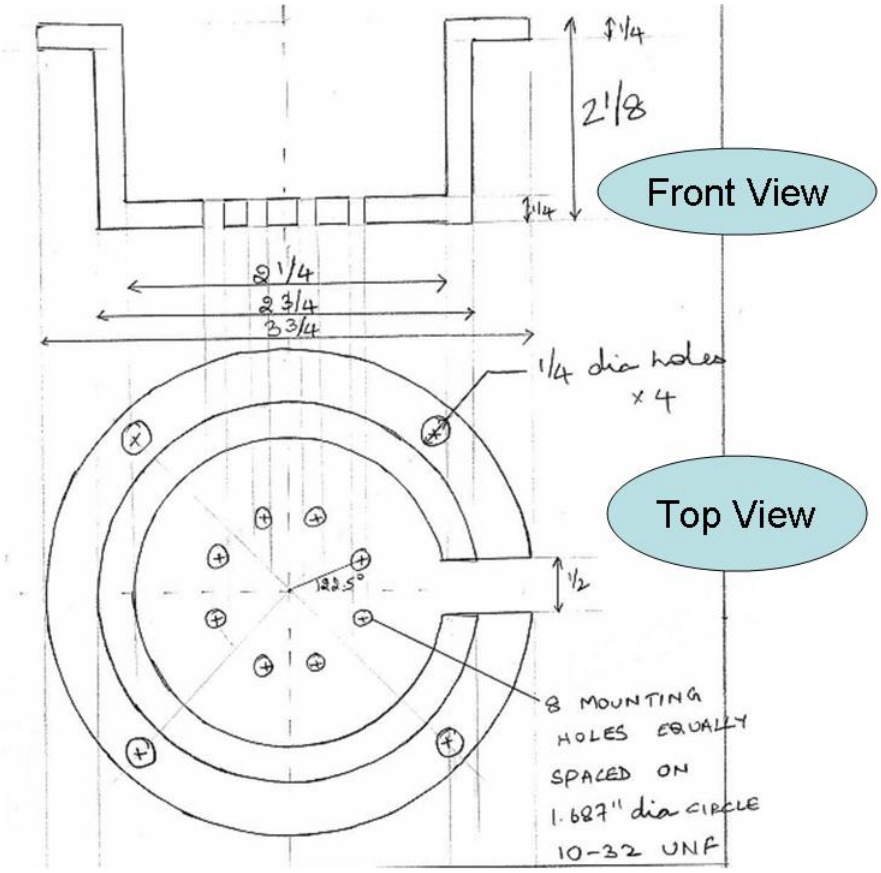

Figure 5.4 Load cell cup holder

The cup holder as shown in Figure 5.4 was machined out of stainless steel. The circular cross section of the holder measured 53.97 mm in length, 57.15 mm inside diameter, 95.25 mm outside diameter and 6.35 mm in thickness. It had 8 mounting holes threaded on the bottom side. These holes matched with the holes on the load cell. A 12.7 mm groove was cut on the side to pass out load cell cable. Four holes each of 6.35 mm diameter were drilled on the flange or lip of the holder. The holder cap had four matching holes.

The load cell cap was a flat circular plate measuring 95.25 mm in diameter and 3.17 mm in thickness. It had a concentric hole at the center measuring 12.7 mm for the stud as shown in Figure 5.5. The cap had four 6.35mm holes corresponding to those on the cup holder.

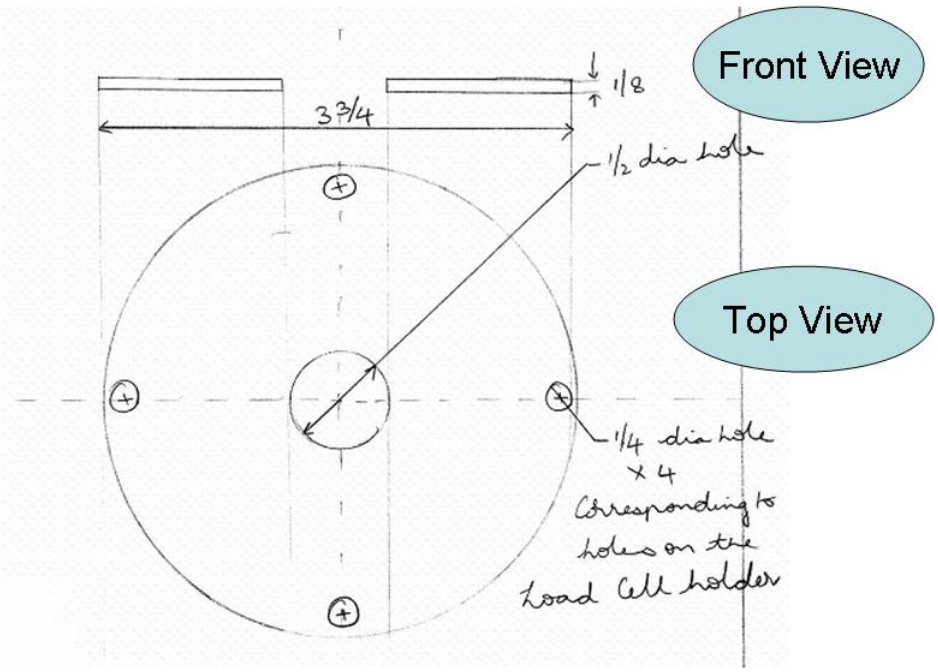

Figure 5.5 Load cell cap

The load cell stud consisted of two parts (a) the stud base which was screwed to the load cell stud and (b) stem which rises up into the mill through the mill shell and the lifter bar. The base was 12.7 mm in inside diameter and 19.05 mm in outside diameter. It measured 15.87 mm in length. The stem was 9.52 mm in diameter and 77.79 mm in length. The top 6.35 mm portion of the stem was threaded. A bell shaped nut was screwed on the stem.

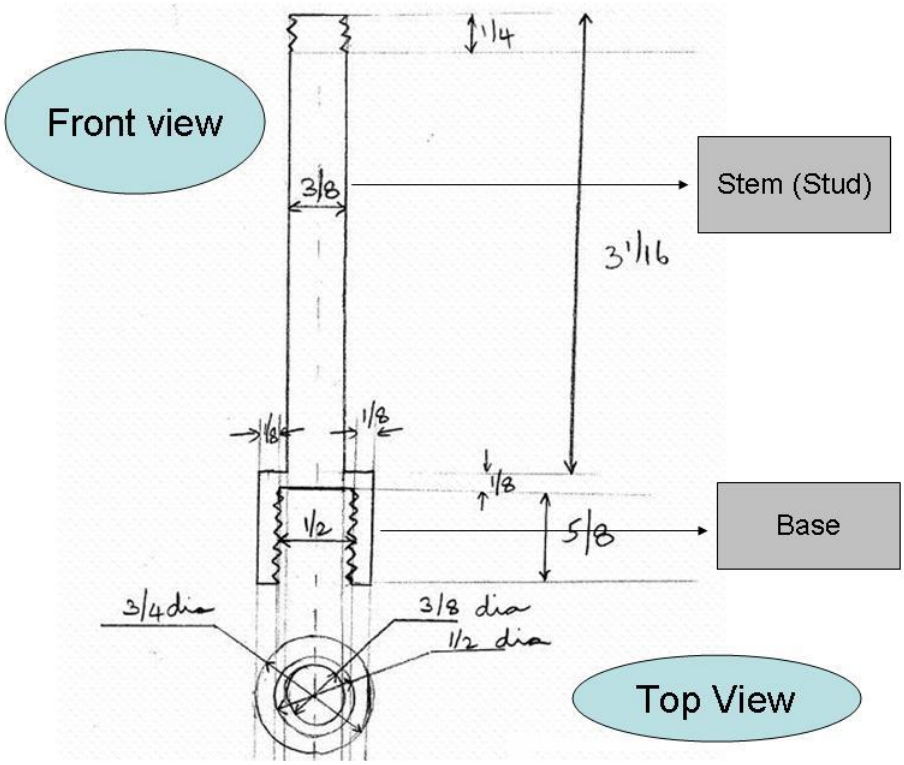

Figure 5.6 Load cell stud

The union of the cup holder, the cap and the stud with the load cell inside is shown in Figure 5.7

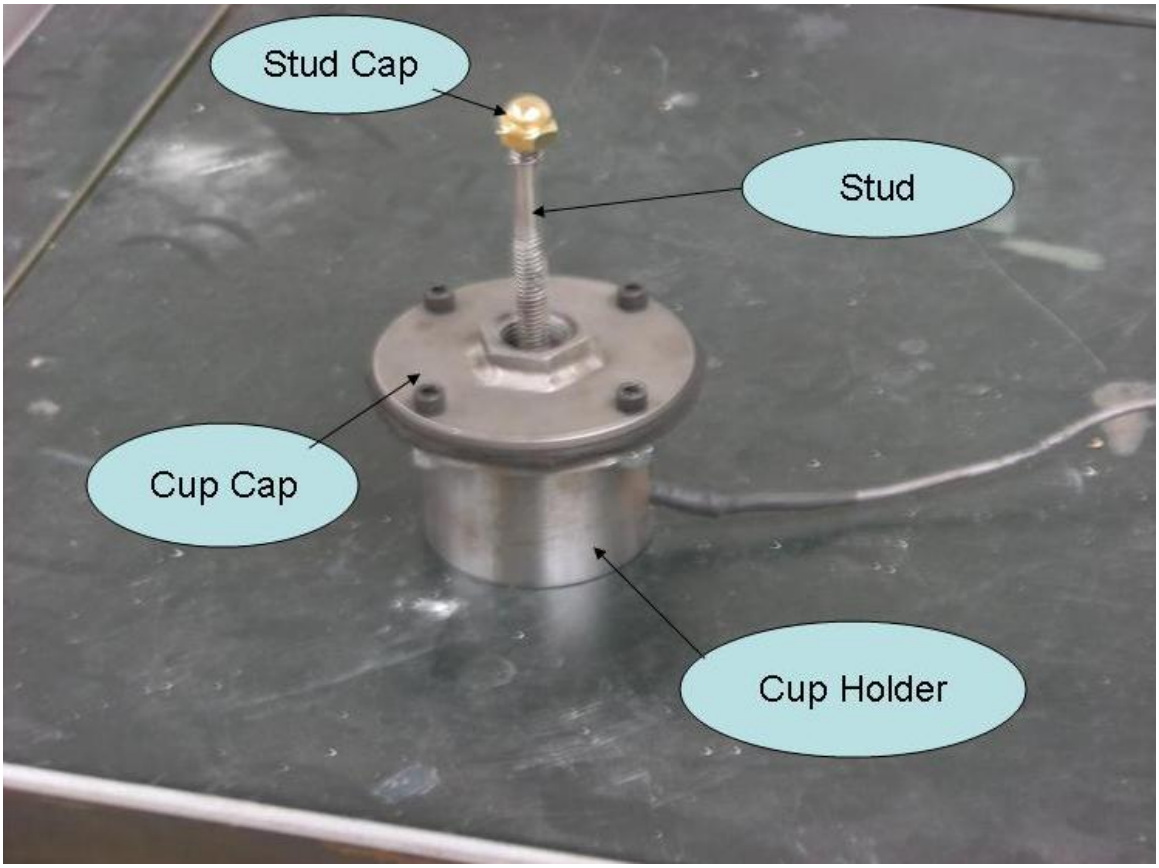

Figure 5.7 Load cell Package

5.1.1.3 Load cell package on the mill shell

The load cell package was attached to the outer side of the mill with only the stud being exposed inside. A half inch hole was drilled on the mill shell and the lifter. The stud on the load cell passed through this hole to the mill interior. On the exterior side of the mill shell, a half inch nut was welded and a corresponding half inch nut was welded on the top side of the cap. A half inch coupling was used to hold the load cell holder to the mill shell. One side of the coupler was screwed onto the nut on the load cell cap and the other side was screwed to the nut on the mill shell. The nuts on each side were perfectly centered so that the stud would not touch the mill shell or the lifter. The diameter of the bell shaped nut on the stud was bigger that the 0.5 inch hole drilled on the mill and the lifter. So the load cell package was attached from the outside and the stud cap was screwed on to it from inside. When there is a hit on the stud cap inside the mill, it will tend to push the load cell backwards which will eventually try to push the load cell cup holder. But since the cup holder is attached to the cup cap which is attached to the mill shell through the coupler, the backward movement of the entire package is restricted. Hence each impact was captured successfully. The load cell wires had to be run to the grate plate as the electronics were all attached to it. To run it from outside, the path was interrupted by the roller bearings on either side of the mill. So, it had to be reintroduced into the mill to reach the grate plate. For this purpose a 10 mm hole was cut on the mill shell and a 10 mm groove was cut into the lifter running parallel to its length. On the

discharge end of the mill, the same slip ring and amplifier assembly was used as before. The package attached to the mill is shown in Figure 5.8.

Figure 5.8 Load cell package attached to the mill

Figure 5.9 Groove in the lifter

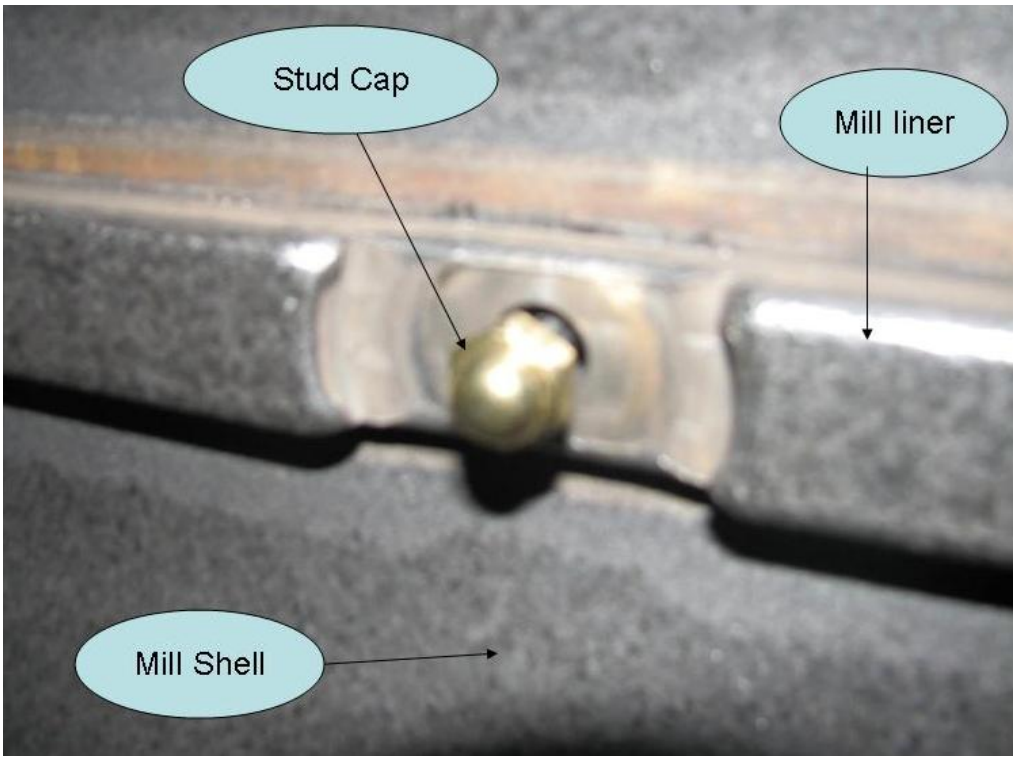

Figure 5.10 Stud cap exposed inside the mill

5.1.2 Experimental Procedure

Several experiments were performed to determine the effect of mill filling, mill speed and the ball size on the impact spectra. The experiments were all run in dry conditions. The experimental design is summarized in Table 5.1.

Table 5.1 Operating Variables

Design Variables	
Ball Size	1 inch, 1.5 inch and 2 inches
Mill Speed	60% to 95% in increments of 5%
Mill filling	10%, 20% and 30% by volume

5.1.2.1 Experimental Procedure to determine the impact of mill speed

1. The mill was filled with 1.5 inch diameter balls to 15% mill filling.
2. The load cell package was fitted from the outside with the stud cap screwed from inside and the mill was closed.
3. The wires were all connected. The same LabView program used earlier for the data acquisition was used here.
4. The mill speed was set at 60% and the mill was turned on.
5. The mill was run for 100 revolutions and the impact data was collected during this period.
6. The mill was then stopped and the connections were all rechecked.
7. The mill speed was increased to 65% and the data was collected for 100 revolutions again.
8. The above steps were repeated as the speed was increased to 95% in steps of 5%.

5.1.2.2 Experimental Procedure to determine the impact of mill filling

1. The mill was filled with steel balls of 1.5 inch diameter to 10% mill filling.
2. The mill was run and the data was collected for 100 revolutions at 60%, 70% and 80% mill speed.
3. The mill filling was increased to 20% and then to 30% and at each mill filling the data was collected at 60%, 70% and 80% mill speed.
4. Between each experiment the electrical connections were checked repeatedly.

5.1.2.3 Experimental Procedure to determine the impact of ball size

Three different ball sizes of 1, 1.5 and 2 inch were used to study the effect of ball size. At each ball size, the mill filling was varied as 10%, 20% and 30% by volume at each mill filling the speed was changed as 60%, 70% and 80% critical speed. For each run, the same procedure mentioned above for the 1.5 inch ball was followed.
The test conditions are summarized in Table 5.2.

Table 5.2 Test Conditions

Variable	Test ID	Ball size (inch)	Mill filling (%)	Mill speed (%)
Speed	A – 501	1.5	15	60
Speed	A – 502	1.5	15	65
Speed	A – 503	1.5	15	70
Speed	A – 504	1.5	15	75
Speed	A – 505	1.5	15	80
Speed	A – 506	1.5	15	85
Speed	A – 507	1.5	15	90
Speed	A – 508	1.5	15	95
Mill Filling	A – 509	1.5	10	60
Mill Filling	A – 510	1.5	10	70
Mill Filling	A – 511	1.5	10	80
Mill Filling	A – 512	1.5	20	60
Mill Filling	A – 513	1.5	20	70
Mill Filling	A – 514	1.5	20	80
Mill Filling	A – 515	1.5	30	60
Mill Filling	A – 516	1.5	30	70
Mill Filling	A – 517	1.5	30	80
Ball Size	A – 518	1	10	60
Ball Size	A – 519	1	10	70
Ball Size	A – 520	1	10	80
Ball Size	A – 521	1	20	60
Ball Size	A – 522	1	20	70
Ball Size	A – 523	1	20	80
Ball Size	A – 524	1	30	60
Ball Size	A – 525	1	30	70
Ball Size	A – 526	1	30	80
Ball Size	A – 527	2	10	60
Ball Size	A – 528	2	10	70
Ball Size	A – 529	2	10	80

Ball Size	A – 530	2	20	60
Ball Size	A – 531	2	20	70
Ball Size	A – 532	2	20	80
Ball Size	A – 533	2	30	60
Ball Size	A – 534	2	30	70
Ball Size	A – 535	2	30	80

In effect, the experiments were done in a 3 variable factorial design.

5.1.3 Results

Very promising and encouraging results were obtained with the new load cell package. The impact spectra clearly showed a movement with each of the variables, particularly mill speed and the ball size. For each experiment, the data set was processed with MATLAB and the force histogram and force spectrum were calculated and plotted.

5.1.3.1 Comparison with Speed

To determine the effect of mill speed on the impact spectra, the mill speed was changed from 60% to 95% with an increment of 5% each time. Other mill conditions were kept constant with ball size at 1.5 inch and the mill filling at 15% by volume. The results are presented in Table 5.3.

Table 5.3 Effect of Mill speed

Force Range (N)	Mill Speed as percentage of critical speed							
	60%	65%	70%	75%	80%	85%	90%	95%
0-200	10563	8216	7627	7498	6021	5589	4156	1948
200-400	4241	3308	3106	2453	2234	1900	1433	705
400-600	141	135	363	120	148	118	199	90
600-800	30	21	34	40	55	49	80	45
800-1000	17	9	11	26	29	22	46	20
1000-2000	25	31	20	41	34	68	71	61
2000-3000	7	11	7	27	8	36	17	5
3000-4000	0	1	0	17	4	5	3	0
40000-5000	0	0	0	11	0	0	0	1
>5000	0	0	0	12	0	3	0	0

Graphical comparison is in Figure 5.11.

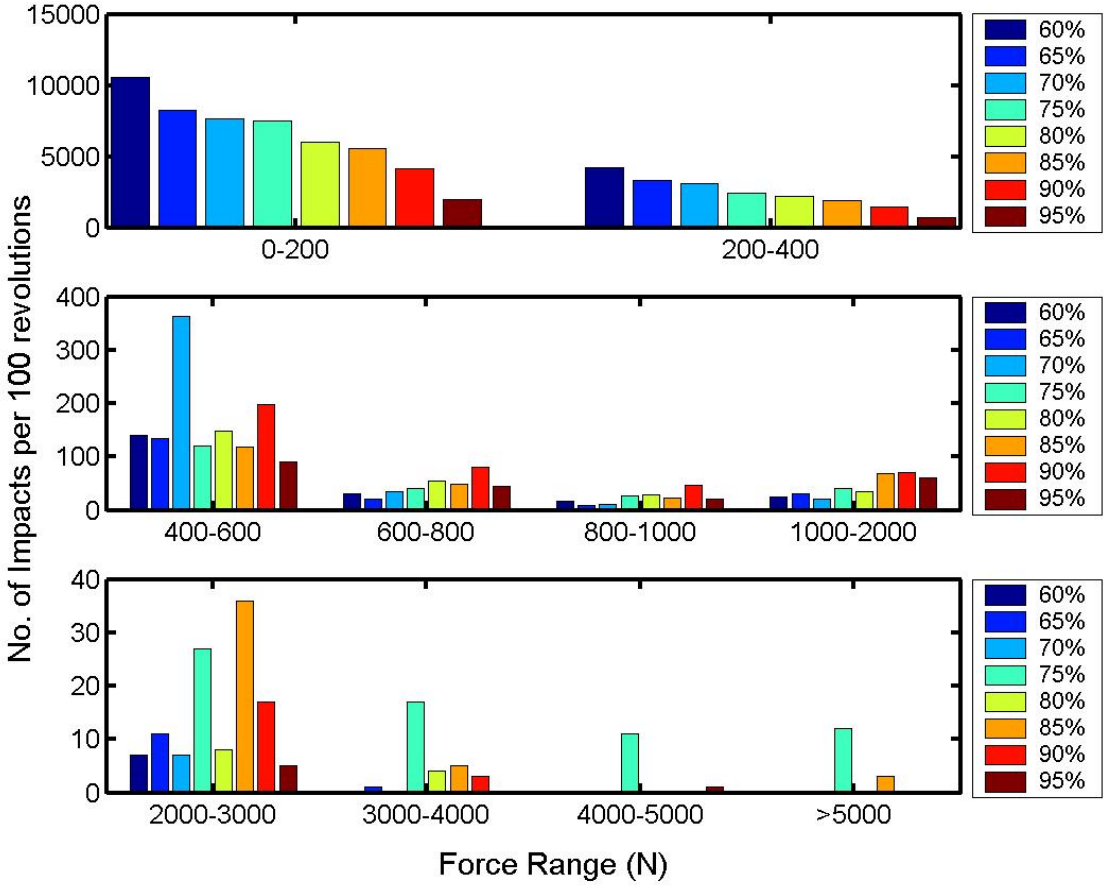

Figure 5.11 Comparison of Impact spectra with mill speed at 15% mill filling and 1.5 inch ball size

As can be seen from the plot, the number of impacts in lower force ranges is maximum at lower speeds. In these force ranges (0-200 N and 200-400 N), the number of impacts decrease with an increase in speed. In the lower speeds of 60% and 65%, the charge generally is in cascading motion. In cascading motion, the charge tends to roll down to the toe of the mill leading to abrasive comminution. So, the forces occurring in this regime is typically weak. This behavior of the charge is clearly exemplified in the above impact spectra where the number of low force hits decrease with an increase in the speed.

At about 65% - 70% the charge motion slowly shifts from a cascading to a cataracting motion and remains in this condition till about 80% to 85% critical speed. In cataracting motion, the grinding ball is projected from the lifter bar to follow a parabolic path before landing on the toe of the charge. This cataracting leads to comminution by impact and hence high force of impact. This behavior was also captured by the impact spectra. In the plot, the numbers of impacts in higher force ranges (above 400 N) are always higher at around 70% speed. As the force range increases the number of impacts at 60% and 65% speed decreases.

At very high mill speeds of about 85% and 90%, the charge begins to centrifuge inside the mill shell, i.e, it is essentially carried around in a fixed position leading to few

impacts. So the total number of impacts in all force bins at high speeds in always low as can be seen in the graph.

5.1.3.2 Comparison with mill filling

Mill filling is one of the most important variables from the operational point of view. The mill filling was varied as 10%, 20% and 30% by volume for study. At each filling, the speed was varied as 60%, 70% and 80% critical speed. The mill filling was varied for three different ball sizes of 1 inch, 1.5 inch and 2 inch. So, effectively 27 different data sets were produced. The data at 70% speed for all three different ball sizes is shown in Table 5.4.

Table 5.4 Effect of mill filling

Force Range (N)	Ball Size = 1 inch			Ball Size = 1.5 inch			Ball Size = 2 inch		
	10%	20%	30%	10%	20%	30%	10%	20%	30%
0-200	11282	10138	8782	8992	8764	8841	4925	4571	3850
200-400	874	846	481	2168	2274	2298	2372	2469	1840
400-600	27	32	22	371	377	418	281	208	464
600-800	3	1	6	65	57	70	53	59	139
800-1000	5	3	3	24	16	25	28	52	47
1000-2000	4	3	7	21	22	22	37	99	68
2000-3000	0	0	5	5	3	5	18	30	14
3000-4000	0	0	1	0	0	5	7	13	5
4000-5000	0	0	0	1	0	1	2	5	4
>5000	0	0	1	1	0	0	8	28	8

Graphic representation of the data for 1.5inch ball size is shown in Figure 5.12.

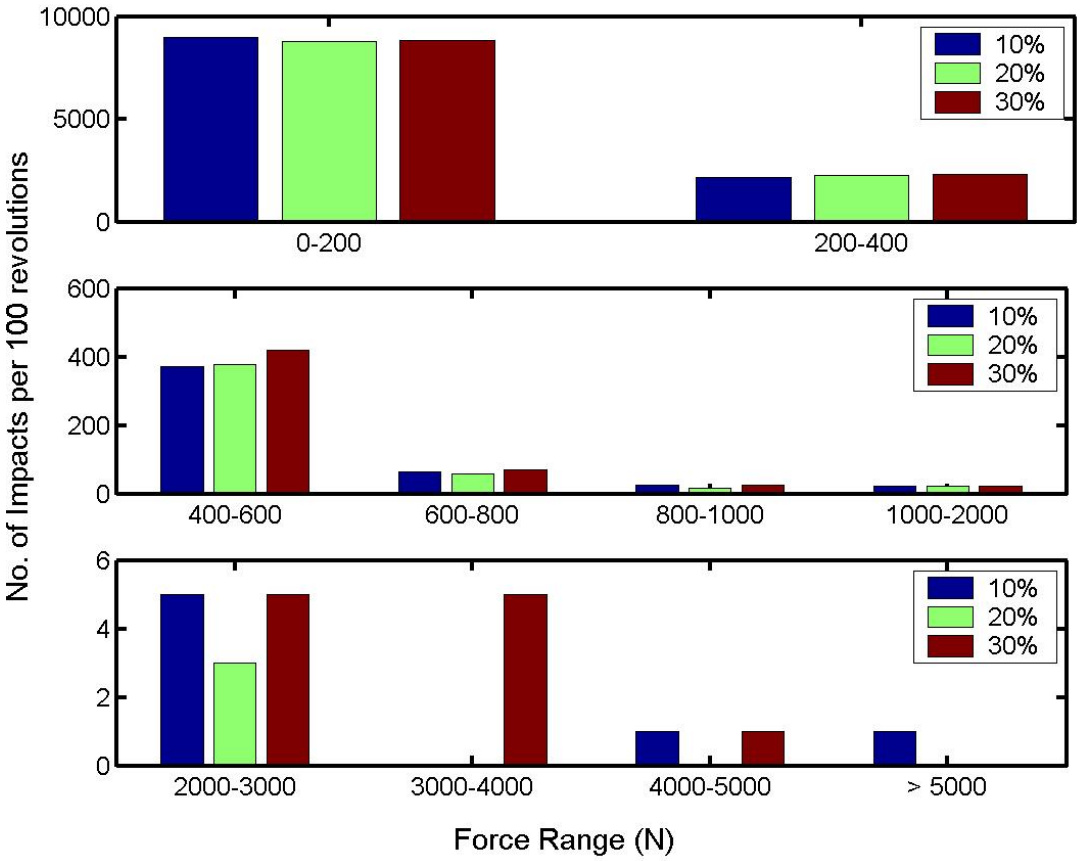

Figure 5.12 Comparison of impact spectra with mill filling using 1.5 inch ball size and at 70% mill speed

As can be seen from the plot above, the impact spectra does change with mill filling. However the change pattern could not be analyzed exactly. The nature of change in impact spectra using 1.5 inch ball is not the same as 1inch ball size which is not same as 2 inch ball. It is predicted that more significant changes in the mill filling, such as 40%, 60% etc, would show dramatic and logical impact trends. This task could not be accomplished to the desired effect due to restriction of availability of the number of balls. It also appears from the data analysis that the mill filling has an interaction effect with mill speed on the impact spectra. The plots generated using 1inch and 2 inch balls are presented in the appendix.

5.1.3.3 Comparison with ball size

For better understanding of the variation in the impact spectra with ball size, a mono-size distribution was used. The first set of experiments was conducted with 1.5 inch ball size. Then the ball size was changed to 1 inch and 2 inch. At each size, the mill filling was varied as 10%, 20% and 30% and at each particular mill filling the speed was changed to 60%, 70% and 80% critical speed. The data is shown in Table 5.5

Table 5.5 Effect of ball size

	Mill filling = 10%			Mill filling = 20%			Mill filling =30%		
Force Range (N)	1inch	1.5inch	2inch	1inch	1.5inch	2inch	1inch	1.5inch	2inch
0-200	11282	8992	4925	10138	8764	4579	8782	8841	3850
200-400	874	2168	2372	846	2274	2469	481	2298	1840
400-600	27	371	281	32	377	208	22	418	464
600-800	3	65	53	1	57	59	6	70	139
800-1000	5	24	28	3	16	52	3	25	47
1000-2000	5	24	37	3	22	99	7	22	68
2000-3000	0	5	18	0	3	30	5	5	14
3000-4000	0	0	7	0	0	13	1	5	5
4000-5000	0	1	2	0	0	5	0	1	4
>5000	0	1	8	0	0	28	1	0	8

The plot of comparison of impact spectra with ball size is shown in Figure 5.13.

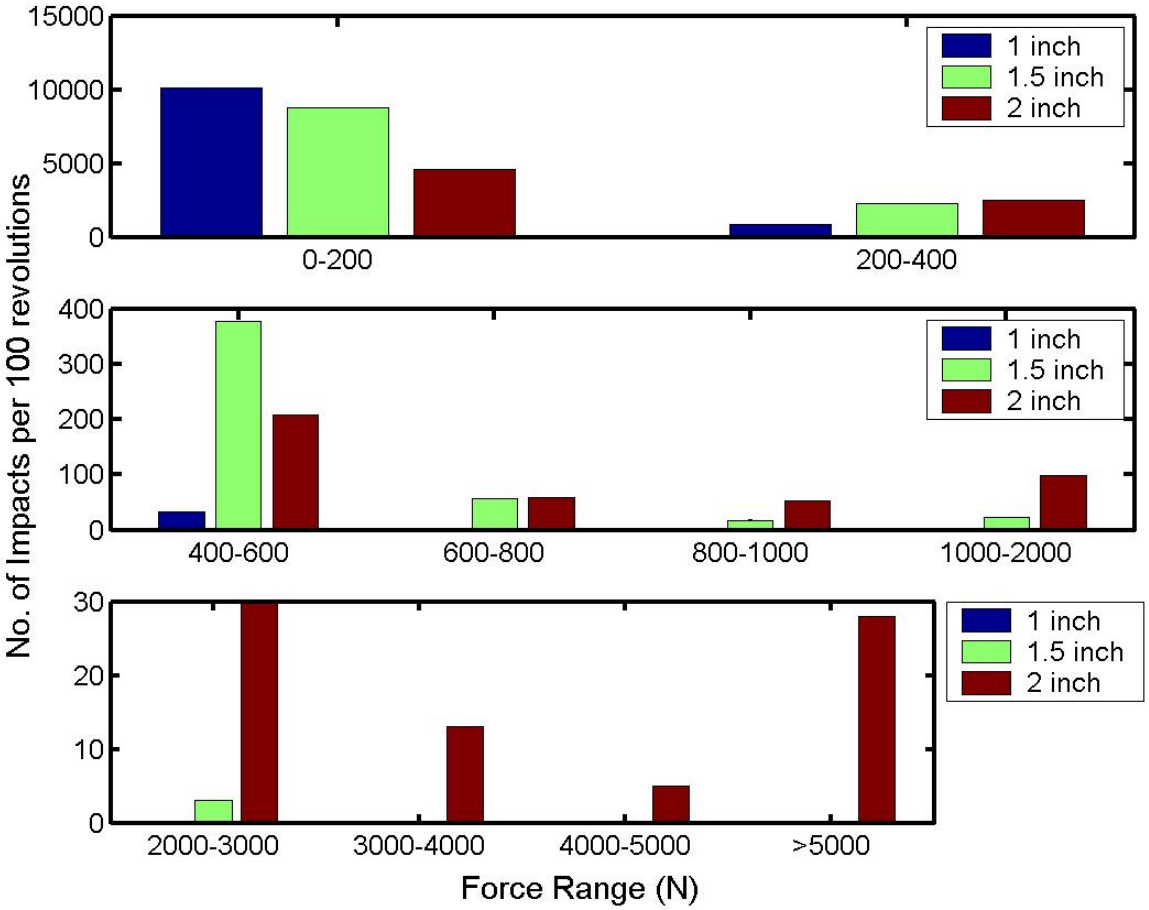

Figure 5.13 Comparison of impact spectra with ball size at 20% mill filling and 70% mill speed

A very clear relation was found between the impact spectra and the ball size. When using bigger ball size, for the same level of mill filling the actual number of balls will drastically decrease by the order of ball size to the power of one third. So, the number of impacts will automatically decrease due to lesser number of balls. But since the ball volume increase by the cube of the diameter, the weight tremendously increases and hence the force of each impact. So, with ball size the total number of impacts will decrease but the average force of each impact will increase. This is precisely what was found from the results. In lower force ranges, the number of impacts is high for smaller ball size but as the force range increases the numbers of impacts tremendously increase with bigger ball. For instance, at 20% mill filling and 70% speed, the number of impacts in the 0-200 N force range using 1 inch ball is 10138 while the number of impacts using 2 inch ball is 4579. But at a higher force range of 5000 N and greater, the number of impacts with 1 inch and 2 inch ball are 0 and 28 respectively. Irrespective of the mill filling or the mill speed, the same relation was found for ball size with impact spectra.

5.1.4 Discussion

The strong relation found between the impact spectra and operating variables has tremendous potential for mill optimization. In a day to day commercial facility, the mill throughput cycles high to low and back over a 12 hour period. The mill operator intuitively diagnoses the problem and corrects water addition to the mill, ore feed rate, ball charge addition or mill speed. This variation in mill throughput can be minimized by using the impact spectra rather than by operator's intuition. Suppose an impact spectra is captured at 6:00 am on Monday when the mill is running at the designed capacity using a ball size of 2 inch. This spectrum will look like the short line starting at about 4500 impacts (blue line) in Figure 5.14. In the week after, the ball size may have decreased to about 1.5 inch diameter and the impact spectra would look like the long line starting at 10000 impacts (green line). By comparing the first impact spectra second one, we will be able to suggest the kind of change that occurred in the charge and hence will be in a position to suggest remedial operating variable changes, like in this case increasing the ball size.

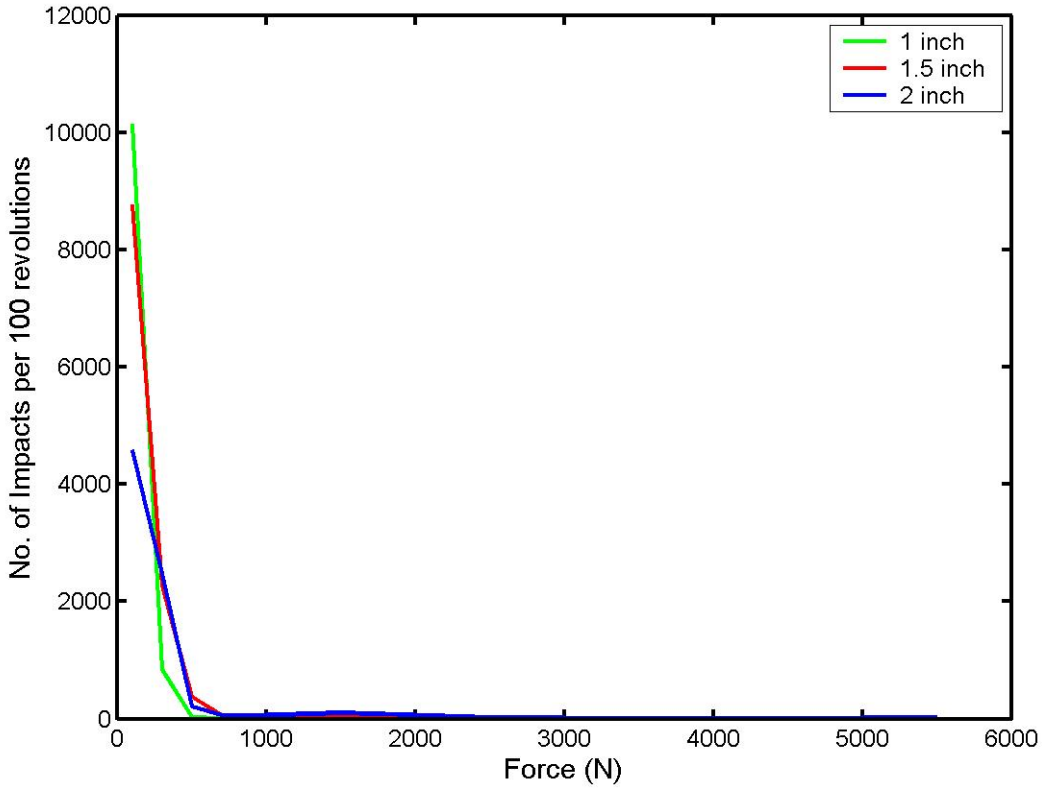

Figure 5.14 Analysis of change in impact spectra with ball size

By understanding and analyzing impact spectra, we will be in a position to make appropriate changes can be made in the operating mill, may it be ball size, ball distribution, speed or mill filling. Thus it can prove to be a very vital tool for mill optimization.

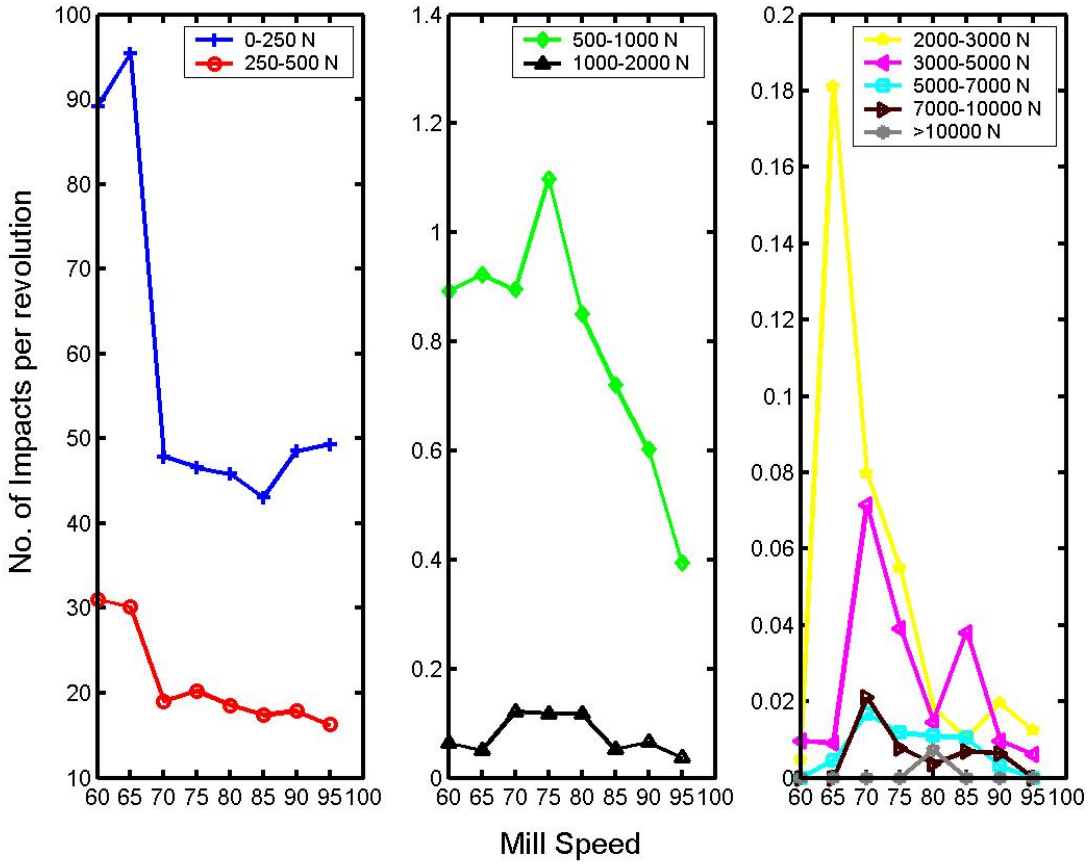

Figure 5.15 Comparison of Impact Spectra with mill speed in different force bins

Figure 4.10 gives a different perspective of the same behavior explained above. It can be seen from this figure as well that in lower force bins 0-250 N and 250-500 N, the number of impacts per revolution decreases with an increase in mill speed. As the force range increases, the number of impacts is always maximum around 70%-80% mill speed. It can also be seen from Figure 4.10 that for a constant mill speed, the number of impacts always decrease as the force range increases. In other words, the number of impacts at any given speed is highest in the 0-250 N bin and least in the 12000-15000 N bins with a progressive decrease from one bin to the other.

6 PLANT TRIALS AT CORTEZ GOLD MINES

6.1 Load cell Package design and design revisions

6.1.1 Concept – Design 1

In any tumbling mill, the breakage of particles occurs in the grinding chamber. The optimal design of shell lifters can produce an efficient charge motion. Once the discharge grate and pulp lifters are designed properly for the required mill capacity, they

would perform consistent with the overall design. However, the milling conditions inside the grinding chamber keep changing. The change `is mainly due to the mine variables and wearing of shell liners (lifters) with time. Till date these uncontrollable and dynamic variations are interpreted based on the power draft and in some operations with accelerometers placed external to the mill. More recently, mill sound recording is also being used to infer the dynamics of the mill online. All these techniques are the indirect ways of measuring the conditions inside the mill.

The original idea was to machine a large (5-6 inch) ball with a central cavity of sufficient size to accommodate strain gauge based load cell, telemetry electronics and a lithium ion battery. This instrumented ball will be charged into a mill. During regular operation, an FM-transmission receiver antenna and computer will receive the signal from the ball. The PC will produce a time history of impacts and impact energy spectra. The ball will continue to transmit the data until all the battery power is used up and/or damage to the electronics resulting in destruction of the ball.

Unfortunately, the current generation radio technology does not support the concept. Even with the most sophisticated modern communications devices it is impossible to transmit a wireless signal from inside the huge mill. The signal would be absorbed in the steel charge and die. A thorough study was done and a wide variety of commercial radio communications companies were contacted but in vain. A number of professors working in this field were consulted and after considering their expert comments and suggestions it was considered to change the design of the package.

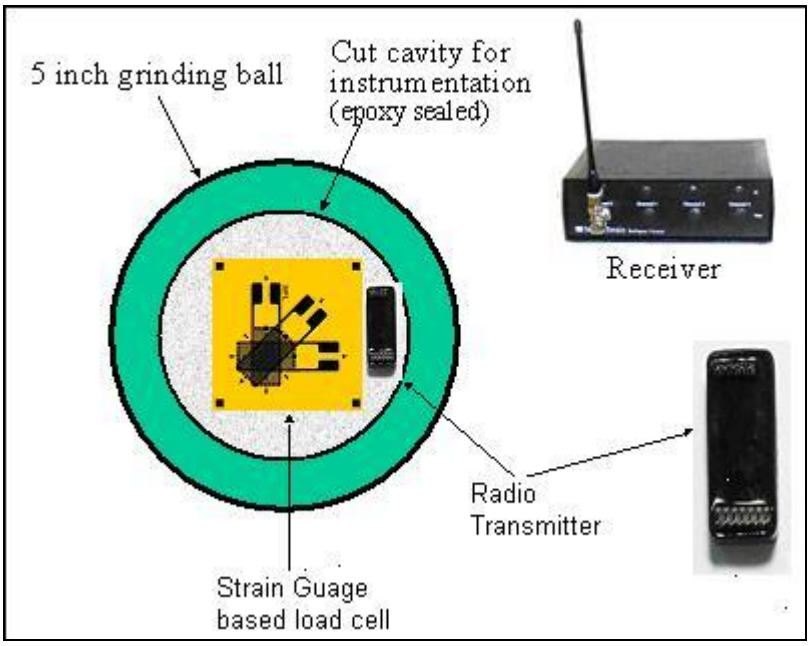

Figure 6.1 Original concept of Instrumented Grinding Ball

6.1.2 Revision -1/Design -2

Due to the above mentioned constraints the concept in all was not abandoned but was modified to still produce the same end result. It was impossible to transmit the wireless signal from inside the mill but it was very much feasible to transmit them from the mill shell. The new design was to fit a load cell package to the liner of the mill and bring its signal to the exterior of the mill in a hard wired fashion which could then be transferred using wireless technology.

A load cell package as described in chapters 3 and 4 was designed accordingly. The package consisted of a load cell, load cell cup holder, cup cap and a floating cap. To calibrate the load cell package, the UFLC was used. Several drop ball experiments were conducted on the load cell and the UFLC for this purpose. The load cell package was placed on the UFLC rod and the ball was dropped on it to mock the UFLC drop ball conditions. A comparison of force profiles recorder by both the devices was done and an excellent correlation was found between the two.

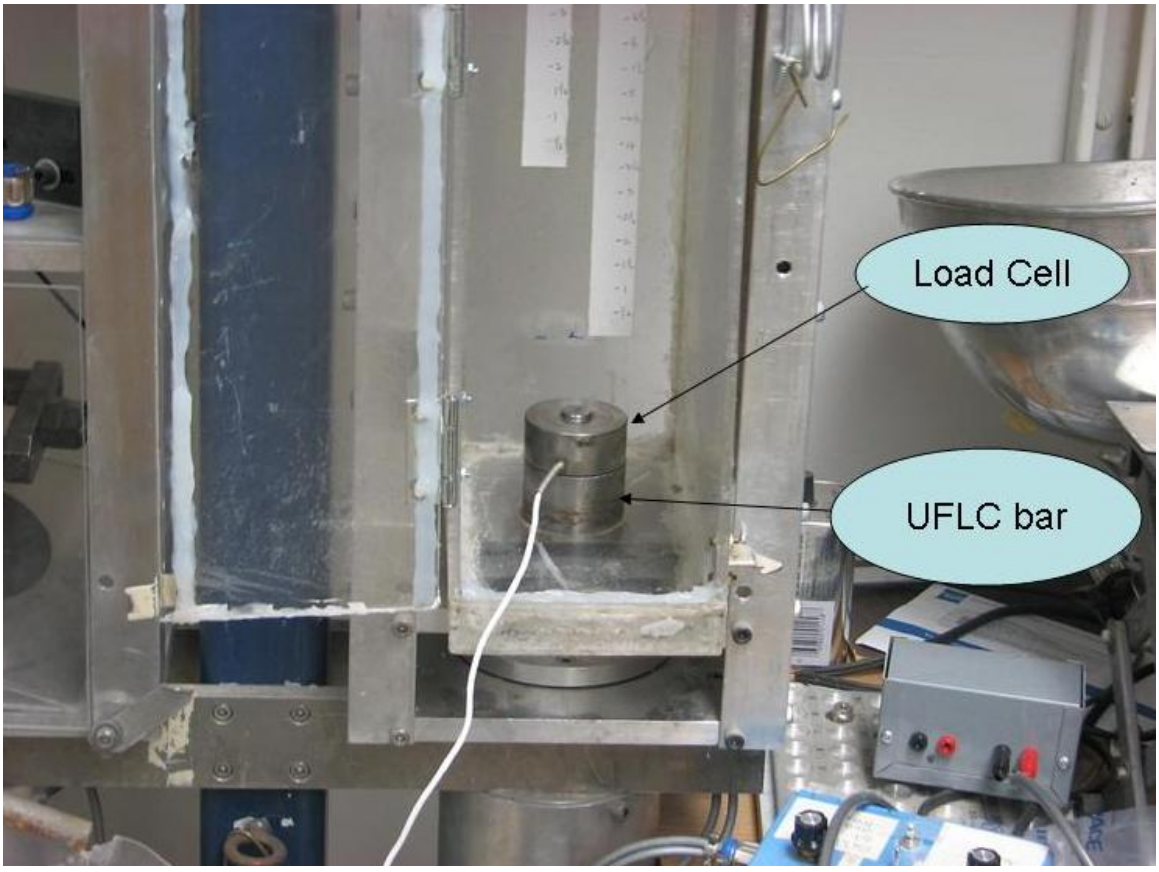

Figure 6.2 Load cell package on the UFLC

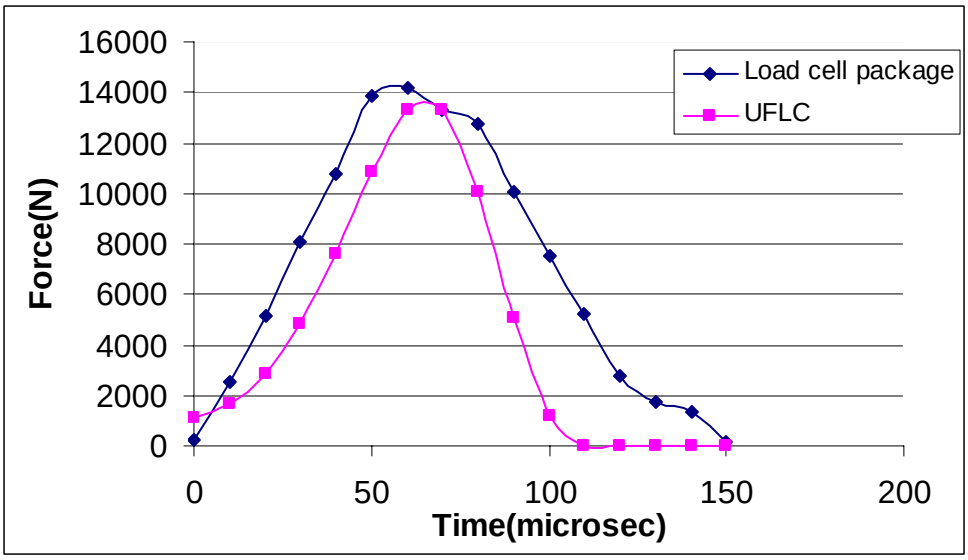

Figure 6.3 Comparison of force profiles when a 1.6 inch ball was dropped from 7 inch height on the UFLC and the load cell package

As it can be seen from Figure 6.3, the force profile of the load cell package closely follows the profile of the UFLC. Convinced with this result, the load cell package was used in the lab scale ball mill and then the pilot mill to produce impact spectra. In both the mills hard wired connections were used to transmit the signals. The signal was transferred with the help of amplifier and slip ring as described earlier. Several experiments were performed changing the mill speed and ball size to investigate their relationship with impact spectrum in a lab scale ball mill and a pilot mill. The experimental design and the results obtained were discussed in detail in chapters 3 and 4.

6.1.3 In house built Wireless Kit

A single impact event occurs in about 100 to 200 microseconds. To get a representation of the complete event at least one sample has to be captured in every 10 microseconds. So, the sampling rate has to be a minimum of 1 sample/10 microseconds or 10^5 samples/second. Using a decent data encryption rate of 10 bits/sample the sampling rate will be equivalent to 10^6 bits per second (bps) or 1000 kbps. So, the minimum data transmission rate of the wireless kit has to be 1000 kbps. There was no commercial wireless kit available that would transmit at this extremely fast rate. There was no commercial vendor available either who would custom make a wireless kit to match the required rate. So, an in-house wireless kit was built here at the University of Utah with the aid of a certified electronics and communications engineer.

The setup consisted of a transmitting module and a receiving module. The transmitting module was made of an amplitude modulator and the receiving end, a demodulator.

6.1.3.1 Wireless circuit test at Cortez Gold Mines

The wireless kit was tested at the Cortez Gold Mines (CGM) concentrator located in Crescent valley, NV. The plant treats 10,000 tons of gold ore per day with a tonnage of 450 tons per hour. Single SAG mill in close circuit with pebble crusher was installed in the plant. It also had a ball mill in open circuit.

The main idea of the exercise was to check for the kind of interference that would be met on the shop floor. A drop ball experiment was designed for this purpose. A 1.5 inch diameter steel ball was dropped from 2 feet height on the load cell package for five consecutive times. The load cell package was connected to the transmitter which would send the signals in wireless mode in real time to the receiver. The load cell package was kept at three different positions on the shop floor each time at 15 feet from the receiver. The receiver end of the kit was kept stationary at one point on the floor. It was connected to a computer for data acquisition. It was at equidistance from SAG mill and the ball mill about 25 feet from either. The load cell package was moved to Position A (5 feet from SAG mill), then to Position B(5 feet from ball mill) and c) 15 feet from the receiver end in opposite side from both the mills. The shop floor plan is shown in Figure 6.4

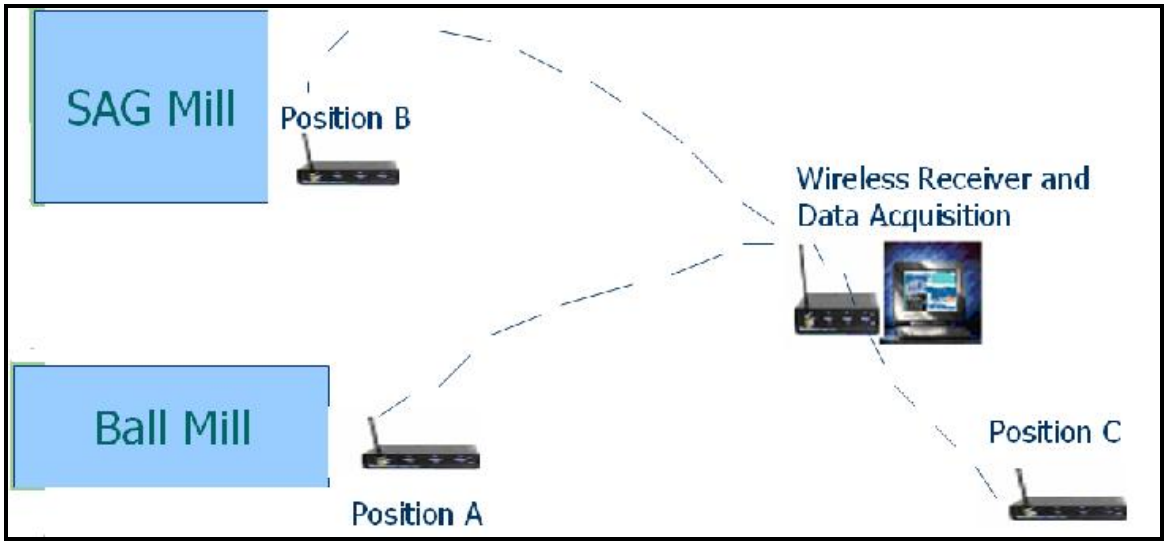

Figure 6.4 Layout of tests on the shop floor at CGM, Nevada

As mentioned earlier, at each position the drop ball test was conducted five times for statistical comparison. The result was found to be statistically reasonable. It is shown in Figure 6.5.

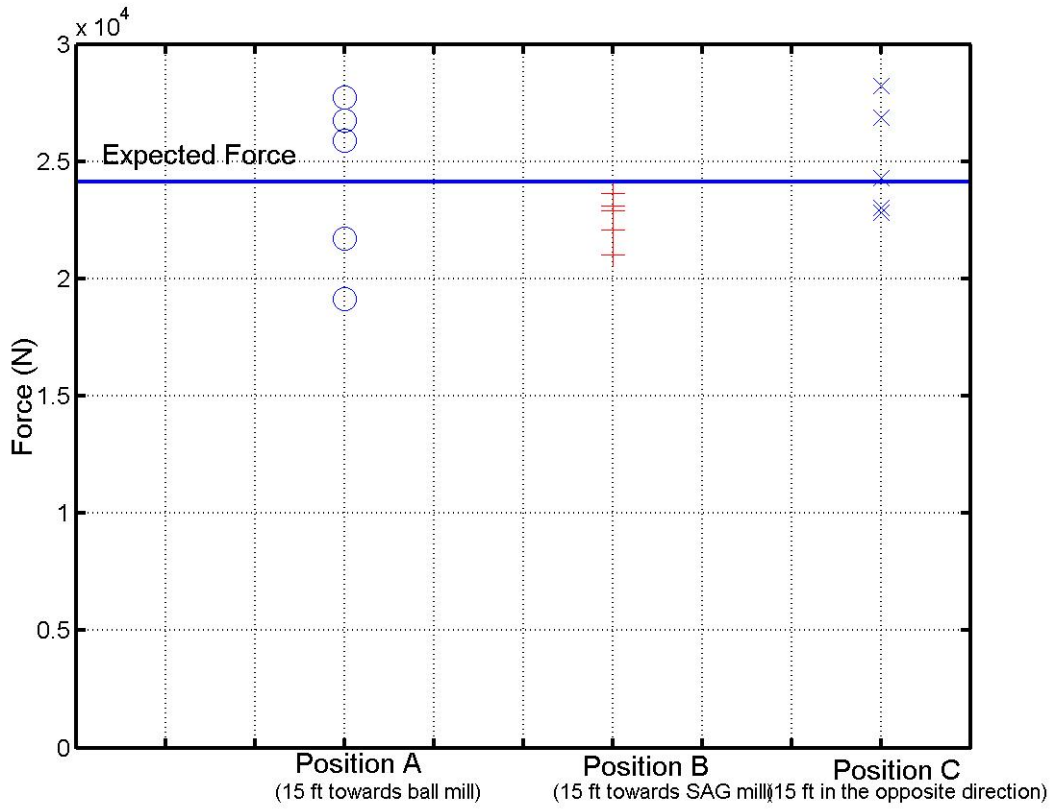

Figure 6.5 Comparison of force at different positions on the shop floor

The theoretical calculation of the force produced when a 1.5 inch ball is dropped from 2 inch height is 25000 N. It can be seen from the plot above that at a) at every position, the force experienced each of the five times is pretty close to one another b) the magnitude of the force is around 25000 N which is the true theoretical force. The little disturbance in the force values is due to some loose connections here and there in the circuit. Looking at the data it would be reasonable enough to say that the noise can be eliminated if the wireless circuit is made precisely by a professional and packaged in the right manner. It is estimated that this would produce data which would be in the ballpark of +/- 100 N. With the partial success of the wireless circuit even at the industry level, the efforts were now concentrated on further refining the load cell package design.

6.1.4 Noise in the Signal

In the current design, the load cell package was fitted to the mill liner from inside. In the running condition of the mill, there are a lot of vibrations in the mill produced from several sources. These mostly arise due to impacts occurring on the mill shell and due to the rotation of the mill. These vibrations propagate throughout the mill shell. So, even when the load cell package does not experience a direct impact due to a colliding ball it stills produces a signal due to vibrations passing through the mill shell to the load cell package. These signals, though are noise, are recorded as impacts.

To investigate this, a new experiment was designed. As part of this, the load cell package was taken out of the mill and was clamped to the mill frame. A 1.5 inch diameter ball was dropped on the frame from a height of 5 inch at a distance of 2, 4, 6, 8 and 10

inch from the load cell package. A strong signal of about 700-1000 N was seen in the load cell. This confirmed the observation made earlier that the vibrations in the mill shell produced a signal which was recorded as impact.

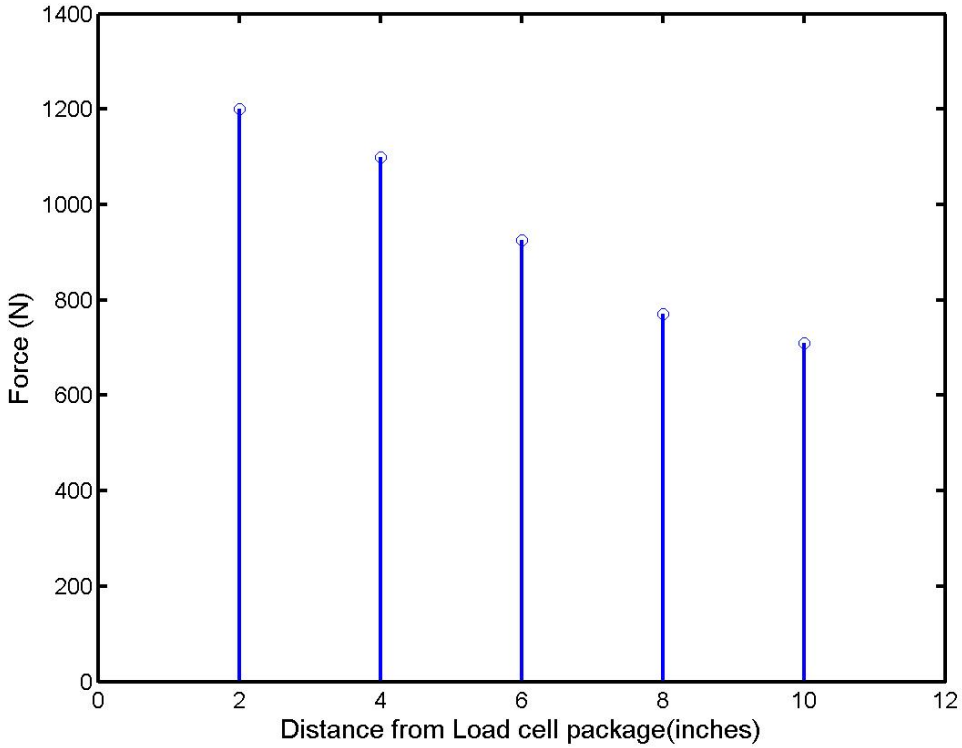

Figure 6.6 Force signals produced due to noise

To further investigate the noise, the impacts were studied with the position of the load cell package in the mill. When the load cell package was at 12 ‘O’ clock position inside the mill the data acquisition was turned on. Data was collected for 5 consecutive revolutions of the mill. The mill was run empty without any charge in it. The result obtained is shown in Figure 6.7

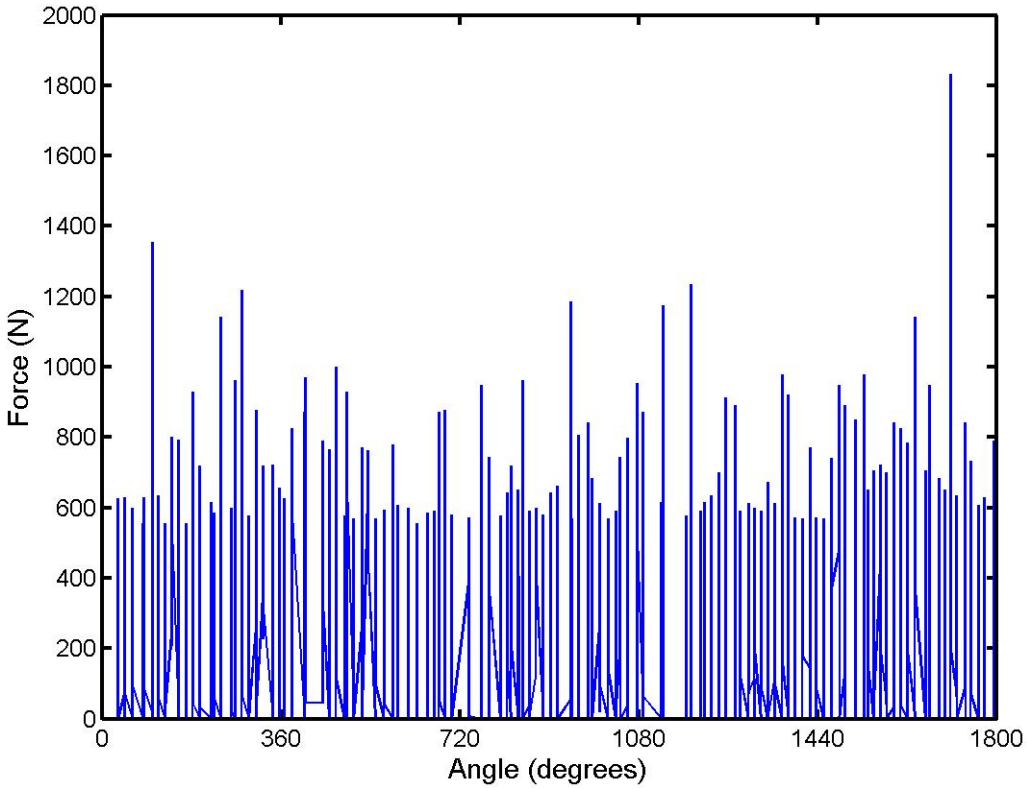

Figure 6.7 Noise signals produced vs. angle of the load cell package in an empty mill

Ideally there should be no signals produced by the load cell package as there is no charge in it but an average signal of 400 N was observed. This clearly goes to prove the point that the vibrations in the running mill get recorded as false impacts. This behavior is exemplified when there is charge in the mill. At any point of time, the multiple impacts of steel balls on the mill produce more vibrations in the mill which in turn produce more noise and more false impact signals in the load cell. Eventually, it was considered to change the design of the load cell package to address this issue.

6.1.5 Load cell package Design -3/Revision -2

The current load cell package design had two major constraints:

- With the load cell sitting inside the mill on the shell liner it would not be possible at the industrial level to bring the load cell cable outside the mill undamaged. For this purpose the design of the liner has to be changed which would not be possible from a practical point of view.
- The load cell package picked up noise due to vibrations in the mill shell as described in the previous article.

To accommodate for these two reasons, the load cell package design was changed substantially. In the new design, the load cell package was placed external to the mill and attached to it by a half inch pipe. A special stud was made that was connected to the load cell on one end and at the other end was exposed inside the mill. Any impact on the stud

inside the mill would be eventually transmitted to the load cell and get recorded. A detailed design of the new load cell package was explained in chapter 5.

Several designs of the stud cap were tried with special importance to two particular types. One of them was a flat circular plate shaped design. This measured 0.5 inch in thickness and 2 inch in diameter with a central groove through which it was screwed to the stud. The other was a bell shaped nut as shown in Figure 6.8. It was found during drop ball experiments that any off center hit on the flat circular nut jammed the threading at the center where it was screwed to the stud. Also, these off center impacts were not transmitted to the load cell without signal attenuation. The bell shaped nut was free of both these concerns and hence was used for the experiments.

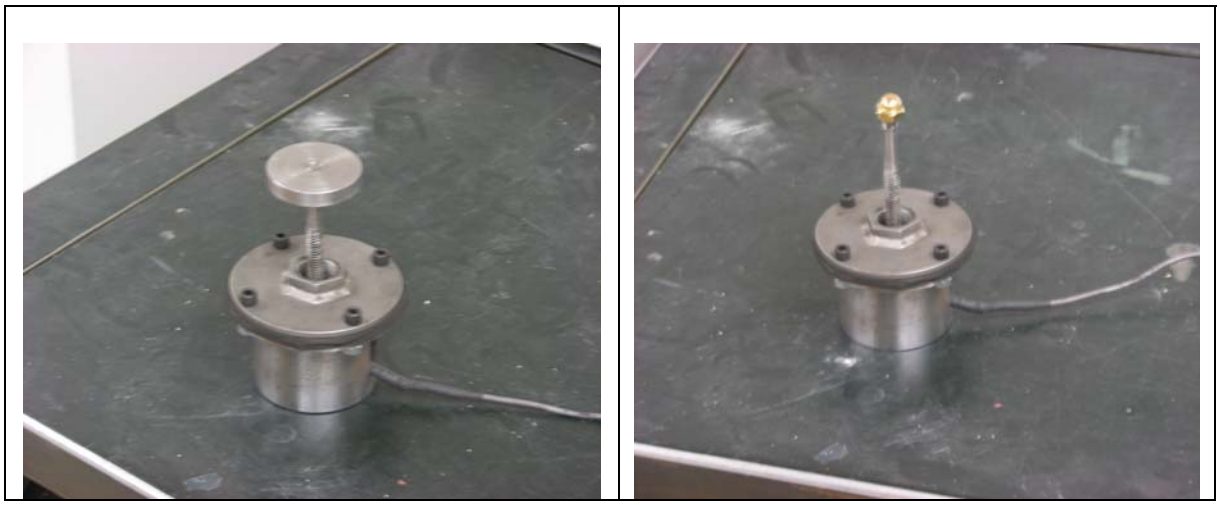

Figure 6.8 (a) Flat circular nut (b) Bell shaped nut

6.1.5.1 Calibrating the new load cell package

With the design change and the fact that the load cell package was no longer experiencing direct impacts, it was important to re-calibrate it. The actual impact now occurred on the stud cap and had to pass through the stud cap and the stud to reach the load cell. There was a potential for the compression wave to be partially absorbed at various weak spots like, the stud cap and the stud threading, stud and the load cell threading. Drop ball experiments were performed for this purpose again. The experiments were designed to get a statistically right factor using three different set of balls - 0.642kg, 0.252kg and 0.124kg. Each ball was dropped from five different heights – 1, 2, 3, 4 and 5 inch. To compare the load cell signal with the load cell package signal 15 drop ball experiments were to be performed on each. The aim of this particular design was to eliminate any human error. The threading on the load cell stud would be easily damaged had it experienced 15 direct impacts. This could viable considering the fact that each load cell costed about $450.00. So, a special flat nut was made to fit the load cell stud as shown in Figure 6.9. The load cell with the flat nut was first calibrated against the load cell.

Figure 6.9 Flat nut to protect the load cell stud

Table 6.1 Calibration of the load cell with load cell + flat nut

Drop Height	Load cell (without cap)	Load cell (with flat nut)	Ratio
1 inch	-1.1556824	-0.652252429	0.564387
2 inches	1.7783195	-0.996845667	0.560555
3 inches	-2.3207405	-1.204860333	0.519171
4 inches	-2.7115138	-1.4474755	0.533826
5 inches	-3.071302667	-1.639856923	0.533929
		Average	**0.542373**
		Standard Deviation	**0.019351**

The load cell + flat nut combination was used to calibrate it against the load cell + stud + stud cap combination. It can be seen in Table 6.1 that standard deviation is as close to zero as it can be. So the calibration factor 0.542373 was conveniently accepted.

Table 6.2 Calibration of the load cell + flat nut with load cell + stud + stud cap

Drop Height	Load cell (With flat nut)	Load cell (With Stud + Cap)	Ratio
0.642 kg ball			
1 inch	-0.652252429	-0.7230994	1.10862
2 inches	-0.996845667	-0.9672608	0.97032
3 inches	-1.204860333	-1.2484754	1.0362
4 inches	-1.4474755	-1.5131288	1.04536
5 inches	-1.639856923	-1.6617268	1.01334
		Average	**1.03477**
		Standard Deviation	**0.05045**

0.252 kg ball			
1 inch	-0.495111571	-0.423530167	0.85542
2 inches	-0.808664333	-0.691366333	0.85495
3 inches	-0.996613333	-0.831110833	0.83394
4 inches	-1.199705333	-0.953331167	0.79464
5 inches	-1.346681167	-0.9954855	0.73921
		Average	**0.81563**
		Standard Deviation	**0.04936**
0.124 kg ball			
1 inch	-0.337879	-0.3158085	0.93468
2 inches	-0.4732425	-0.526740833	1.11305
3 inches	-0.609354	-0.558815	0.91706
4 inches	-0.724282455	-0.63312	0.87413
5 inches	-0.8205962	-0.6713005	0.81806
		Average	**0.9314**
		Standard Deviation	**0.11106**
		Grand Average	**0.927265**
		Grand Standard Deviation	**0.116325**

The standard deviation at each of the balls was 0.05045, 0.04936 and 0.11106, which are low enough to be accepted. The overall standard deviation was 0.116325. The calibration factor between load cell + flat nut combination and load cell + stud + stud cap combination was thus determined as 0.927265.

The overall calibration between new load cell package and load cell = calibration factor between load cell and load cell + flat nut combination x calibration factor between load cell + flat nut combination and load cell + stud + stud cap.

= 0.542373 x 0.927265

= 0.502924

Hence, actual signal = 1/0.502924 x signal produced by load cell package

= 1.988372 x load cell package signal

6.1.5.2 Noise elimination in the new design

A full scale signal the load cell can produce is about 100,000 N and an average noise signal is about 1000 N which is about 1% of the full scale load cell output. So the interference of noise was completely ignored in the first design of the load cell package. The majority of the impacts in the mill are due to cataracting and these forces are in the range of 500-2000 N. Though the magnitude of the noise signals is not significant the number becomes very significant which was overlooked in the design. Adding to this is the fact that the noise signal corresponds in magnitude to the low force signal. So it was now very vital to eliminate the noise.

The current design was a significant betterment to eliminate noise than its predecessor. It has intrinsic advantages owing to its design. The load cell package was no longer in direct contact with the mill which led to the elimination of more than 90% of the noise. In the previous design, the load cell package was sitting directly on the mill liner. Any vibration in the liner propagated though the load cell cup holder to the load cell. In the current design, the only way a noise signal could reach the load cell was to pass through the pipe connecting the mill and the load cell package. The load cell was isolated form the cup holder except at the bottom where it was screwed. So, the noise in the mill shell has to pass through the pipe, the load cell cap, and load cell cup holder and then through the screws to the load cell. There were three points of connection in its route – the pipe and load cell cap joint, load cell cap and load cell cup holder joint and the load cell cup holder and the load cell joint. Owing to its tenuous route, the noise got attenuated naturally to some extent which acted to our advantage. To further eliminate the noise, a 1/8 inch rubber ring was placed between the cup cap and the cup holder. Also, a special aluminum damping foil 2552, manufactured by 3M was used. This foil was worn around the pipe at the pipe and load cell cap joint. It was also used at the load cell cap and load cell holder joint. So, now only direct impact on the stud cap will be transferred to the load cell and all other noise would be eliminated. To check this, the mill was again run under empty conditions and a force vs. angle of the load cell package analysis was done like before. Data was collected for 5 consecutive revolutions.

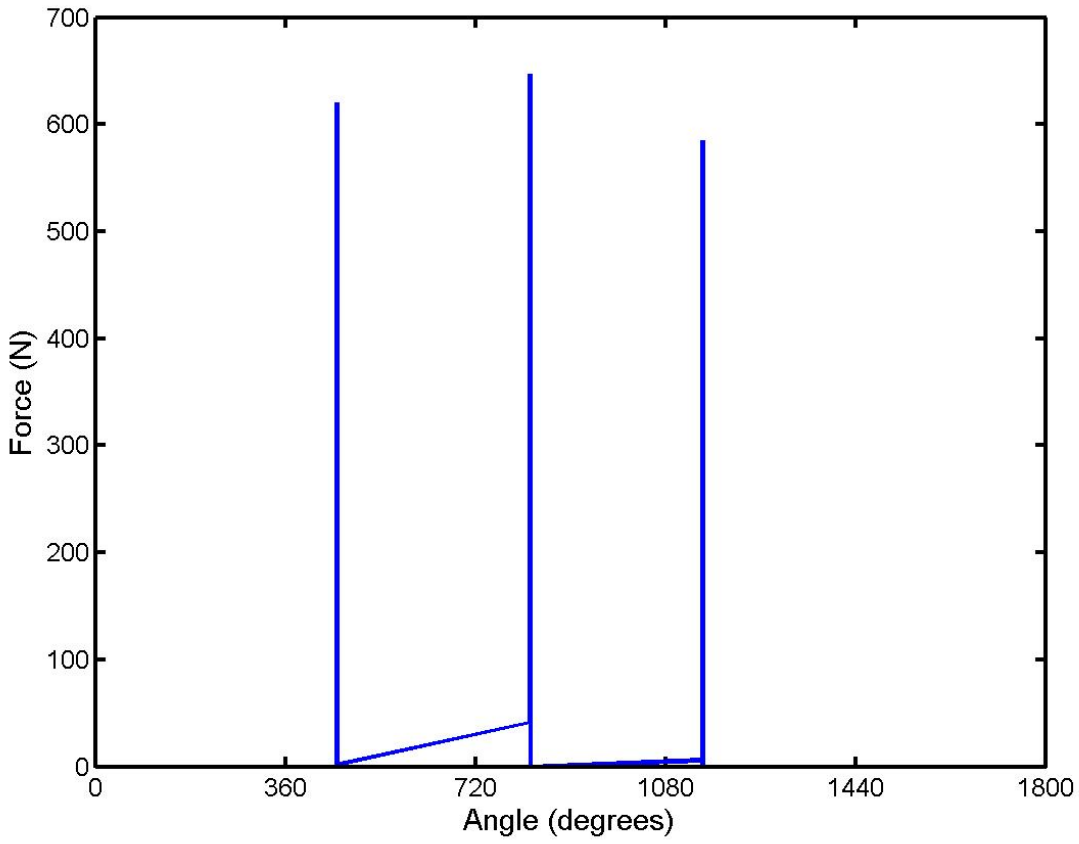

Figure 6.10 Noise signals vs. angle of the new load cell package

In comparison with Figure 6.7 it can be seen in Figure 6.10 that the noise has decreased in leaps and bounds. Convinced with the accuracy of the signals produced by the new load cell package, it was now used to study the effect of the mill operating variables on the impact spectrum in the pilot scale mill.

6.1.6 Proposed design to be used in an industrial scale mill

The current design can be successfully extended to be used in an industrial mill with little modifications. The liners in an industrial scale mill are held against the mill shell using giant size nut and bolts. These measure about 10 inch in length and 3 to 4 inch in diameter, as shown in Figure 6.11.

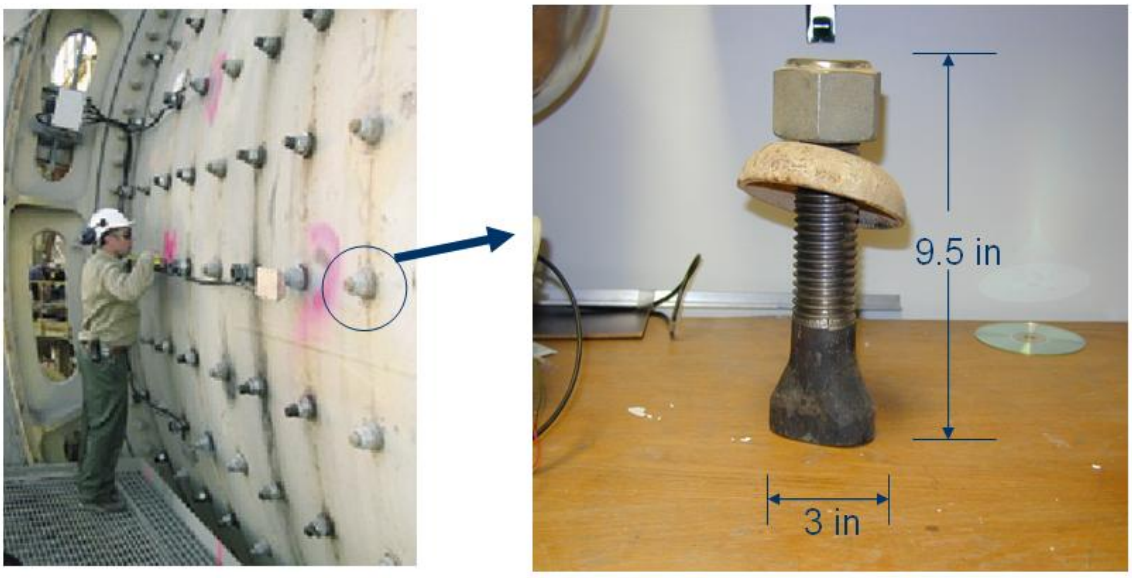

Figure 6.11 Industrial mill bolts

This bolt can be used as the alternative to the pipe in the current load cell package design. The load cell package can be screwed to the bottom side of the bolt. Any impact on the liner will be transferred to the bolt which will eventually be transferred to the load cell. The amplifier and the telemetry electronics can be stuck on the outside of the mill shell adjacent to the load cell package to transmit the signals in real time. However hardening the electronics to sustain on the mill shell might be a challenging issue. The holistic concept is shown in Figure 6.12.

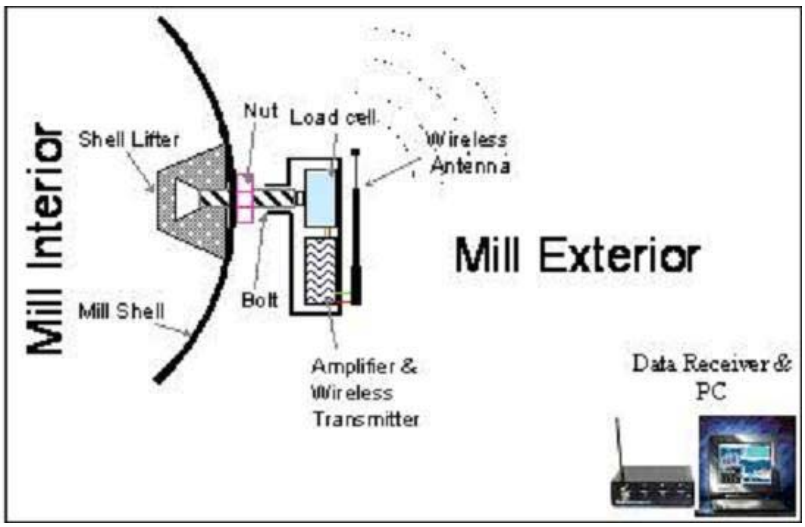

Figure 6.12 Proposed design of the load cell package to be used in industry.